Effective Lagrangian approach to the theory of η photoproduction in the $N^*(1535)$ region

M. Benmerrouche and Nimai C. Mukhopadhyay
Physics Department, Rensselaer Polytechnic Institute, Troy, New York 12180-3590
and Saskatchewan Accelerator Laboratory, University of Saskatchewan, Saskatoon, Saskatchewan, Canada S7N 0W0

J. F. Zhang
Physics Department, Rensselaer Polytechnic Institute, Troy, New York 12180-3590
(Received 20 July 1994)

We investigate η photoproduction in the $N^*(1535)$ resonance region within the effective Lagrangian approach (ELA), wherein leading contributions to the amplitude at the tree level are taken into account. These include the nucleon Born terms and the leading t-channel vector meson exchanges as the nonresonant pieces. In addition, we consider five resonance contributions in the s and u channels; in addition to the dominant $N^*(1535)$, these are $N^*(1440)$, $N^*(1520)$, $N^*(1650)$, and $N^*(1710)$. The amplitudes for the π^0 and the η photoproduction near threshold have significant differences, even as they share common contributions, such as those of the nucleon Born terms. Among these differences, the contribution to the η photoproduction of the s-channel excitation of the $N^*(1535)$ is the most significant. We find the off-shell properties of the spin-3/2 resonances to be important in determining the background contributions. Fitting our effective amplitude to the available data base allows us to extract the quantity $\sqrt{\chi\Gamma_\eta}A_{1/2}/\Gamma_T$, characteristic of the photoexcitation of the $N^*(1535)$ resonance and its decay into the η-nucleon channel, of interest to precise tests of hadron models. At the photon point, we determine it to be $(2.2 \pm 0.2) \times 10^{-1}$ GeV^{-1} from the old data base, and $(2.2 \pm 0.1) \times 10^{-1}$ GeV^{-1} from a combination of old data base and new Bates data. We obtain the helicity amplitude for $N^*(1535) \to \gamma p$ to be $A_{1/2} = (97 \pm 7) \times 10^{-3}$ GeV$^{-1/2}$ from the old data base, and $A_{1/2} = (97 \pm 6) \times 10^{-3}$ GeV$^{-1/2}$ from the combination of the old data base and new Bates data, compared with the results of the analysis of pion photoproduction yielding 74 ± 11, in the same units. The observed differential cross section is not very sensitive to either the nature of the η-nucleon coupling or to the precise value of the coupling constant; we extract a broad range of values for the ηNN pseudoscalar coupling constant: $0.2 \leq g_\eta \leq 6.2$ from our analysis of all available data. We predict, in our ELA, the angular distributions for a critical series of experiments at Mainz, and find them to be in good agreement with the preliminary Mainz data. Finally, we discuss implications for future experimental studies with real photons at the Continuous Electron Beam Accelerator Facility (CEBAF) and other emerging medium-energy electron accelerators. Polarization observables, in particular, invite spécial scrutiny at high precision.

PACS number(s): 13.60.Le, 12.39.−x, 25.10.+s, 25.20.Lj

I. INTRODUCTION

In recent years there has been considerable interest [1], both theoretical and experimental, in the study of the η meson and its interactions with the nucleon. Suggestions [2] have been made for using the η to probe $s\bar{s}$ quark component in the nucleon wave function. Also there is rising interest in the measurement of rare and forbidden decays of η [3] as a test of physics beyond the standard model. In the present work, the focus is on photoproduction of the η meson and the role of production and decay of the $N^*(1535)$ resonance [the so-called $S_{11}(1535)$ in the pion-nucleon phase-shift analysis] of spin 1/2 and odd parity. This resonance has a remarkably large ηN branching ratio, a fact that needs explanation in the theories of hadron structure based on quantum chromodynamics (QCD). It lies only 48 MeV above the ηN threshold, and is the dominant contributor to the photoproduction amplitude even at threshold. In contrast with the low energy πN and KN interactions, where values of scattering lengths imply a repulsive interaction [4], the ηN scattering length obtained in the analysis [5] of $\pi^- p \to \eta n$ suggests an attractive interaction between η and N. More recently, the analysis of the $pp \to pp\eta$ near threshold suggests a possibility of an attractive ηNN interaction and may also lead to the formation of "bound" η-nucleus states [6]. An ideal tool for the study of the $N^*(1535)$ is through electromagnetic processes, as we demonstrate in this work.

The η meson is a member of the ground state SU(3) meson nonet. Thus, the study of η photoproduction, the subject of this paper, shares many of the fundamental motivations of the extensive study of pion photoproduction over the past 20 years or so, including those done at RPI, both theoretically [7–11] and experimentally [12]. These and other related studies have provided an impressive amount of information about the dynamical properties of the $\Delta(1232)$ as an isolated quantum mechanical system, and its behavior inside the complex nucleus. Above this resonance region, however, large background

contributions [13], and the overlapping of higher resonances make studying one specific resonance by pion production mechanisms very difficult. Just as the dominance of the $\Delta(1232)$ in the (γ,π) processes has allowed the extraction of quantitative information on its electromagnetic transition amplitudes, we hope to extract similar information on $N^*(1535)$ via the (γ,η) process [13]. This is an important focus of this paper. These photocoupling amplitudes provide useful tests for realistic hadron models inspired by QCD.

Most of the older data on photoproduction of the η meson on protons come from the experiments done in the late 1960s and early 1970s [14–22]. These have been reviewed by Genzel, Joos, and Pfeil [23], and Baldini [24]. The existing older experimental data are neither very consistent nor complete in kinematic coverage. There are large ranges of photon energies and scattering angles, where no data on differential cross section exist at present. The available old data base on differential cross section on photoproduction [14–22] contains 137 points, most of which are for center of momentum (c.m.) energy below 1.6 GeV. Only one polarization observable, the recoil proton polarization, has been measured [25], but it is too poor (seven data points, of which five are at 90°) to be of much theoretical value. To this, some more data, of limited quantity (15 differential cross-section data points), have been added by Homma *et al.* [26] covering the photon lab energy region from 810 to 1010 MeV. This data set has large energy uncertainties of the order ± 20 MeV and the angular resolution is $\approx \pm 10°$. More recently, members of the Pittsburgh-Boston-LANL Collaboration at Bates [27,28] have been able to measure the angular distribution for the (γ,η) reaction at photon lab energies of 729 and 753 MeV at six angles each. To summarize, the data base for the η photoproduction have not reached the relatively high level of accuracy known for pion photoproduction in the $\Delta(1232)$ region. An equivalent multipole set, crucial in constraining theoretical models, *does not exist.*

With the advent of high-duty cycle electron accelerators, such as the recently upgraded machines at the Bates (MA), Bonn, Mainz, NIKHEF, and particularly, the Continuous Electron Beam Accelerator Facility (CEBAF), just coming on line, systematic and precise studies of the η photoproduction over a wide range of energies, angles, and momentum transfers should become routine.

The first round of experiments at the Mainz Microtron has been completed, and 45 new data points, as yet preliminary, have been added [29] to the data base, covering the photon lab energies from 722 MeV to 783 MeV. This data set has the potential to make the existing data base almost irrelevant in future, because of better energy and angular resolutions, and statistics.

Existing theoretical analyses for the $\gamma p \to \eta p$ reaction are either based on a Breit-Wigner-type parametrization [26,30,31] or coupled channel isobar model [32,33]. However, it is not clear how to interpret the couplings extracted in the latter work, as they yield "bare" couplings that cannot be related to the observable or physical couplings. Most of these models have not only suffered from the crudeness of the data, but also from the lack of enough theoretical constraints in restricting the number of parameters fitted, 24 or more.

Recently, there was considerable excitement over the experiments at Saclay [34] and Mainz [35] on the π^0 photoproduction near threshold. The results first seemed to indicate a dramatic discrepancy between the experimentally determined threshold amplitude [36] E_{0+} and the theoretical prediction [37] based on approximate chiral symmetry [implying a useful low energy theorem (LET)]. This triggered a considerable amount of work [38,39,40,41,42] on possible corrections to the LET. However, careful reanalyses [7,44,45] concluded that there were no significant deviations from the LET prediction for the multipole E_{0+}. Given this intense theoretical discussion on the π^0 photoproduction, the η photoproduction has taken an added interest [13], in view of the large chiral symmetry violation in the case of the η meson.

After the Letter by two of us [13] on the η photoproduction appeared, Tiator, Bennhold, and Kamalov [33] used a tree-level scheme motivated by our work. But there are important differences between our approach and theirs. First, these authors ignore the complexity of the spin-3/2 particles [80], u-channel resonance exchanges [13], etc. Thus, their treatment of the background is quite different from ours. Second, they have focused on the extraction of the η-nucleon coupling constant. However, we do not agree with their primary conclusion that the η photoproduction data determines the η-nucleon coupling quite accurately. This difference is not surprising because of the point (1). As we show below, the η-nucleon coupling constant is not well determined from the data base that we have. We, instead, address here the physics of the $N^*(1535)$. Finally, because of the multiple scattering effects, Tiator *et al.* get bare couplings of the meson-baryon or photon-baryon vertices that cannot be directly compared to hadron model predictions, or to those we extract in our paper.

The main objective of this paper is to study photoproduction of the η meson on protons from threshold through the $N^*(1535)$ resonance region in the effective Lagrangian formalism, with a view to extract the product of the $N^*(1535) \leftrightarrow p$ electromagnetic transition amplitude and the amplitude for the decay of the $N^*(1535)$ via the η-nucleon channel, from the existing data. The remainder of this paper is organized as follows. Section II is concerned with the formalism of photoproduction of the η meson. Kinematics, invariant amplitudes, and multipole expansion are reviewed. Section III introduces the effective Lagrangian formalism and the amplitudes arising from various particle exchanges are given in the tree approximation. This section is devoted to the photoproduction mechanism. Some important theoretical issues associated with the treatment of the spin-3/2 baryons are also examined in this section. Results, followed by a comparison between π^0 and η photoproduction near threshold, are given in the Sec. IV. Section V summarizes our conclusions and poses some future research problems in this area. Appendices provide some details of the theory, helpful for further understanding of the formalism.

In brief, this work explores the tree-level structure of

the η photoproduction in the $N^*(1535)$ region. The overwhelming dominance of the $N^*(1535)$ resonance, demonstrated below, should make the main results obtained in this paper substantially immune from the unitarity corrections, ignored here. The reason for this optimism is that the Breit-Wigner form of the $N^*(1535)$ is already unitary, and other contributions are too small to be of any great consequence in the unitarity violation.

II. GENERAL FORMALISM

In order to fix the notation and the convention [46] basic formulas for kinematics, invariant amplitudes, differential cross section, and other observables are reviewed in this section.

A. Kinematics

In this work, the following reaction of photoproduction of the η meson on a nucleon is considered:

$$\gamma(k) + N(p_i) \to \eta(q) + N(p_f), \tag{1}$$

where for each particle we have indicated the four-momentum in parentheses.

Use is made of the usual invariant quantities (Mandelstam variables)

$$\begin{aligned} s &= (k+p_i)^2 = (q+p_f)^2, \\ u &= (k-p_f)^2 = (q-p_i)^2, \\ t &= (q-k)^2 = (p_i-p_f)^2, \end{aligned} \tag{2}$$

subject to the constraint $s+t+u = 2M^2+\mu^2+k^2$, where M and μ denote the masses of the nucleon and the η meson. It is easier to work in the c.m. frame of the final nucleon and the η meson where the experimental observables are calculated. The relations (2), in the c.m. system, become

$$s = W^2 = (E_i + k_0)^2, \tag{3}$$

$$u = M^2 + k^2 - 2\,k_0\,E_f - 2\,|\mathbf{q}|\,|\mathbf{k}|x, \tag{4}$$

$$t = \mu^2 + k^2 - 2\,k_0\,\omega + 2\,|\mathbf{q}|\,|\mathbf{k}|x, \tag{5}$$

$$x = \cos\theta = \frac{\mathbf{q}\cdot\mathbf{k}}{|\mathbf{q}|\,|\mathbf{k}|}, \tag{6}$$

with θ being the c.m. scattering angle and W, the total c.m. energy. It is straightforward to derive the following energies and momenta in terms of W and k^2:

$$k_0 = \frac{W^2+k^2-M^2}{2W}, \quad E_i = \frac{W^2-k^2+M^2}{2W}, \tag{7}$$

$$\omega = \frac{W^2+\mu^2-M^2}{2W}, \quad E_f = \frac{W^2-\mu^2+M^2}{2W}, \tag{8}$$

$$|\mathbf{p}_f| = |\mathbf{q}| = \sqrt{\omega^2-\mu^2} = \frac{\sqrt{[(W-M)^2-\mu^2][(W+M)^2-\mu^2]}}{2W}, \tag{9}$$

$$|\mathbf{p}_i| = |\mathbf{k}| = \sqrt{k_0^2-k^2} = \frac{\sqrt{[(W-M)^2-k^2][(W+M)^2-k^2]}}{2W}, \tag{10}$$

where

$$\begin{aligned} k &= (k_0, \mathbf{k}), \quad p_i = (E_i, -\mathbf{k}), \quad q = (\omega, \mathbf{q}), \\ p_f &= (E_f, -\mathbf{q}). \end{aligned} \tag{11}$$

For photoproduction, $k^2 = 0$, and the relation between the energy E_γ of the photon in the lab frame and the c.m. energy is

$$E_\gamma = \frac{W^2-M^2}{2M}. \tag{12}$$

The threshold for the photoproduction of the η meson is at the photon lab energy of 709.3 MeV, corresponding to a W of 1487.1 MeV. These contrast with the corresponding values for the neutral pion of 144.7 and 1079.1 MeV.

B. Invariant amplitudes

The S-matrix elements for the elementary processes (1) can be written as [48]

$$S_{fi} = \frac{1}{(2\pi)^2}\delta^4(p_f+q-p_i-k)\sqrt{\frac{M^2}{4\omega k E_i E_f}}\,i\mathcal{M}_{fi}. \tag{13}$$

The invariant matrix element $i\mathcal{M}_{fi}$ can be decomposed as

$$i\mathcal{M}_{fi} = \bar{U}(p_f)\varepsilon_\mu O^\mu U(p_i), \tag{14}$$

where $U(p_i), \bar{U}(p_f)$ are the Dirac spinors for the initial and final nucleon, respectively; O^μ describes the current operator produced by the strongly interacting hadrons, and ε_μ is the photon polarization vector.

The spin dependence can be made explicit by decomposing the hadron current operator O^μ in terms of eight most general Lorentz covariant pseudovectors:

$$O^\mu = \sum_{j=1}^{8} B_j(s,t,u,k^2)N_j^\mu. \tag{15}$$

Because of the pseudoscalar nature of the η meson, the only Dirac matrices that enter in (15) are γ_5, $\gamma_5\gamma_\mu$, and $\gamma_5\gamma_\mu\gamma_\nu$. Taking into account the Dirac equation for the incoming and outgoing nucleon, both on shell,

$$\gamma\cdot p_i U_i = MU_i, \tag{16}$$

$$\bar{U}_f\gamma\cdot p_f = M\bar{U}_f, \tag{17}$$

and conservation of the four-momentum ($p_i + k = p_f + q$), one can form eight Lorentz pseudovectors $\bar{U}_f N_j^\mu U_i$, where N_j^μ are

$$\begin{aligned} &N_1^\mu = \gamma_5 P^\mu, \quad N_2^\mu = \gamma_5 q^\mu, \quad N_3^\mu = \gamma_5 k^\mu, \\ &N_4^\mu = \gamma_5\gamma^\mu, \quad N_5^\mu = \gamma_5\gamma\cdot kP^\mu, \quad N_6^\mu = \gamma_5\gamma\cdot kq^\mu, \\ &N_7^\mu = \gamma_5\gamma\cdot kk^\mu, \quad N_8^\mu = \gamma_5\gamma\cdot k\gamma^\mu, \end{aligned} \tag{18}$$

where $P^\mu = \frac{1}{2}(p_i + p_f)^\mu$. Any other pseudovector can be reduced to a linear combination of the N_j^μ. The current conservation (gauge invariance) condition $k_\mu j^\mu = 0$, and the identity $k^2 = 0$ reduce the number of independent amplitudes to four for photoproduction [49], where j^μ is the electromagnetic hadron current. These yield the well-known Chew-Goldberger-Low-Nambu (CGLN) [50] amplitudes. The matrix element $i\mathcal{M}_{fi}$ is expanded as

$$i\mathcal{M}_{fi} = \bar{U}_f(p_f)\sum_{j=1}^{4} A_j(s,t,u,k^2)M_j U_i(p_i), \tag{19}$$

where

$$\begin{aligned} M_1 &= -\tfrac{1}{2}\gamma_5\gamma_\mu\gamma_\nu F^{\mu\nu}, \\ M_2 &= +2\gamma_5 P_\mu(q_\nu - \tfrac{1}{2}k_\nu)F^{\mu\nu}, \\ M_3 &= -\gamma_5\gamma_\mu q_\nu F^{\mu\nu}, \\ M_4 &= -2\gamma_5\gamma_\mu P_\nu F^{\mu\nu} - 2MM_1, \end{aligned} \tag{20}$$

with the electromagnetic field tensor

$$F^{\mu\nu} = \varepsilon^\mu k^\nu - \varepsilon^\nu k^\mu. \tag{21}$$

For electroproduction of η, the sum in Eq. (19) is extended to include M_5 and M_6, given by

$$\begin{aligned} M_5 &= \gamma_5 k_\mu q_\nu F^{\mu\nu}\ , \\ M_6 &= -\gamma_5 k_\mu \gamma_\nu F^{\mu\nu}\ . \end{aligned} \tag{20'}$$

The above particular form of the invariant amplitudes exhibits simple properties under crossing symmetry, when the initial and final nucleon are interchanged [48,51]. For the processes under consideration, the crossing (i.e., exchange $s \leftrightarrow u$) properties of the A's can be readily deduced [48,51]:

$$\begin{aligned} A_j(s,t,u,k^2) &= +A_j(u,t,s,k^2) \quad (j = 1,2,4), \\ A_j(s,t,u,k^2) &= -A_j(u,t,s,k^2) \quad (j = 3,5,6), \end{aligned} \tag{22}$$

where we have included also the electroproduction case. The isospin decomposition of the amplitudes is accomplished in the following way. The photon interaction has an isovector part and an isoscalar part, assuming that it has no isotensor part [52]. The vector part leads to isovector amplitudes A_j^V and the scalar part gives isoscalar amplitudes A_j^S. Since the η meson is isoscalar, only isospin $\frac{1}{2}$ final states are allowed. Thus, the isospin decomposition of the amplitudes has the simple form

$$A_j = A_j^S + A_j^V\tau_3\ , \qquad j = 1,...,6, \tag{23}$$

where the two physical amplitudes are given by

$$\begin{aligned} \gamma p \to \eta p:&\ \ A_j^p = A_j^S + A_j^V, \\ \gamma n \to \eta n:&\ \ A_j^n = A_j^S - A_j^V. \end{aligned} \tag{24}$$

C. The CGLN amplitudes

It is convenient to reexpress the invariant amplitudes in terms of amplitudes corresponding to a definite parity and angular momentum state. The matrix elements appearing in Eq. (19) are first written in a two-component form by expressing the γ-matrices in terms of the Pauli σ-matrices, and the Dirac spinors in terms of the two component spinors:

$$\mathcal{M}_{fi} = \frac{4\pi W}{M}\chi_f^\dagger \mathcal{F}\chi_i, \tag{25}$$

where the χ_i, χ_f are the initial and final nucleon Pauli spinors and the factor $\frac{4\pi W}{M}$ has been introduced as a definition of the $\mathcal{F}$. It can be written in the familiar form [51]

$$\begin{aligned} \mathcal{F} &= i\boldsymbol{\sigma}\cdot\mathbf{b}\mathcal{F}_1 + \boldsymbol{\sigma}\cdot\hat{\mathbf{q}}\boldsymbol{\sigma}\cdot(\hat{\mathbf{k}}\times\mathbf{b})\mathcal{F}_2 + i\boldsymbol{\sigma}\cdot\hat{\mathbf{k}}\hat{\mathbf{q}}\cdot\mathbf{b}\mathcal{F}_3 \\ &\quad + i\boldsymbol{\sigma}\cdot\hat{\mathbf{q}}\hat{\mathbf{q}}\cdot\mathbf{b}\mathcal{F}_4, \end{aligned} \tag{26}$$

with $\mathbf{b} = \boldsymbol{\varepsilon}$ for photoproduction. For electroproduction,

$$b_\mu = \varepsilon_\mu - \frac{\boldsymbol{\varepsilon}\cdot\hat{\mathbf{k}}}{|\mathbf{k}|}k_\mu,\ \ \hat{\mathbf{k}} = \frac{\mathbf{k}}{|\mathbf{k}|},\ \ \hat{\mathbf{q}} = \frac{\mathbf{q}}{|\mathbf{q}|}, \tag{27}$$

and two extra terms are to be added to $\mathcal{F}$ in Eq. (26). This extra piece is

$$-i\boldsymbol{\sigma}\cdot\hat{\mathbf{q}}b_0\mathcal{F}_5 - i\boldsymbol{\sigma}\cdot\hat{\mathbf{k}}b_0\mathcal{F}_6.$$

Note that $\mathbf{b}\cdot\mathbf{k} = 0$, so that b_μ has no longitudinal component. The relations between the $\mathcal{F}$'s and the A's is derived by reducing Eq. (19) into two-component spinors. One obtains

$$\begin{aligned} \mathcal{F}_1 &= \frac{ab}{8\pi W}\{(W-M)A_1 + (W-M)^2A_4 + q\cdot kA_{34}\}, \\ \mathcal{F}_2 &= \frac{qk}{8\pi Wab}\{-(W+M)A_1 + (W+M)^2A_4 \\ &\quad + q\cdot kA_{34}\}, \\ \mathcal{F}_3 &= \frac{qkb}{8\pi Wa}\{(W^2-M^2)A_2 + (W+M)A_{34}\}, \\ \mathcal{F}_4 &= -\frac{q^2a}{8\pi Wb}\{(W^2-M^2)A_2 - (W-M)A_{34}\}, \end{aligned} \tag{28}$$

where

$$A_{34} = A_3 - A_4.$$

For electroproduction, $\mathcal{F}_1$, $\mathcal{F}_2$ will have the following extra terms inside the curly brackets: $-k^2A_6$, and $\mathcal{F}_3$, $\mathcal{F}_4$ will have $-k^2A_2/2 + k^2A_5$. And there will be extra amplitudes $\mathcal{F}_5$, $\mathcal{F}_6$ given by

$$\begin{aligned} \mathcal{F}_5 &= -\frac{qa}{8\pi Wb}\{(E_i - M)[A_1 - (W+M)A_{46}] \\ &\quad + [q\cdot k - \omega(W-M)]A_{34} - A_{25}\}, \\ \mathcal{F}_6 &= \frac{kb}{8\pi Wa}\{(E_i + M)[A_1 + (W-M)A_{46}] \\ &\quad - [q\cdot k - \omega(W+M)]A_{34} - A_{25}\}, \end{aligned} \tag{28'}$$

where

$$\begin{aligned} A_{25} &= [\mathbf{q}\cdot\mathbf{k}(\tfrac{3}{2}k_0 - 2W) + |\mathbf{k}|^2(W - \tfrac{3}{2}\omega)]A_2 \\ &\quad - (\omega k^2 - k_0 q\cdot k)A_5, \\ A_{46} &= A_4 - A_6. \end{aligned}$$

Here the notation $k = |\mathbf{k}|$, $q = |\mathbf{q}|$ has been adopted and the definitions $a = \sqrt{E_i + M}$ and $b = \sqrt{E_f + M}$ have been used. By a tedious but straightforward manipulation [53], one can relate $\mathcal{F}_i$ to the multipoles, which are classified according to the nature of the photon and the total angular momentum $J = \ell \pm \frac{1}{2}$ of the final state. The transverse photon states can be electric EL, with parity $(-)^L$, or magnetic ML, with parity $(-)^{L+1}$, where L is the total angular momentum of the photon, $L \geq 1$. The scalar (or longitudinal) photons are relevant for the electroproduction of mesons: the corresponding multipoles are SL, with parity $(-)^L$. The $N^*(1535)$ resonance with spin $J = \frac{1}{2}$ and negative parity, corresponding to $\ell = 0$ of ηN final state, can be excited, with real photons, by the $E1$ radiation. The corresponding multipole would be E_{0+}. For the electroproduction of etas, we would additionally have the scalar multipole S_{0+}. In Sec. III, we shall discuss the nonresonant (Born) and the s-channel $N^*(1535)$ contributions to this multipole, and its difference with that in the case of the π^0 photoproduction.

III. PHOTOPRODUCTION OF THE η MESON

The effective Lagrangian approach [8,54,55] helps us sort out the tree-level structure (Fig. 1) of the η photoproduction amplitude by considering the leading exchanges in the s, t, and u channels. The procedure is exactly parallel to the pion photoproduction. The leading s- and u-channel nucleon Born terms, along with vector meson in the t channel, are added to the contribution of nearby resonances in the s and u channels.

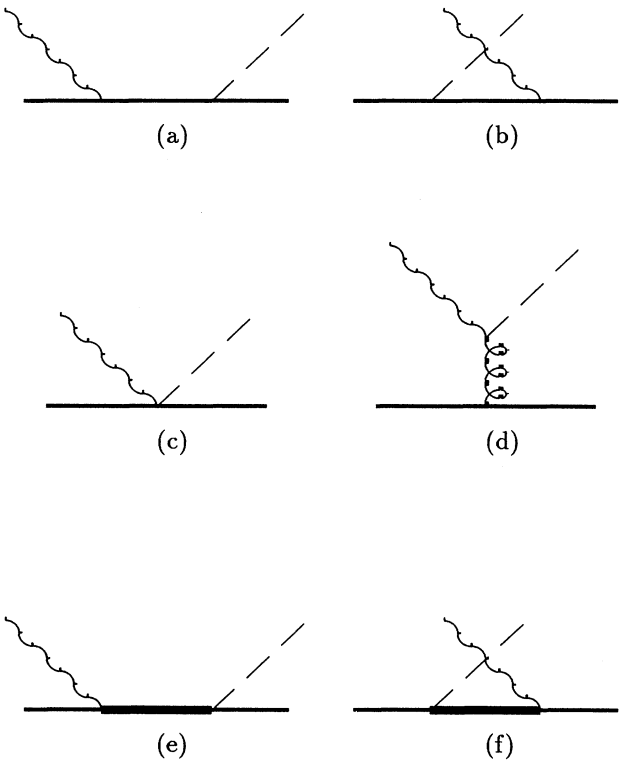

FIG. 1. Feynman diagrams for the η photoproduction. (a), (b) The direct (s-channel) and crossed (u-channel) PS nucleon Born contributions; (c) the equivalence breaking contribution; (d) the t-channel ρ^0 and ω vector meson exchanges; (e), (f) the s- and u-channel nucleon resonance excitations.

A. Nucleon Born terms

In pion photoproduction, the πNN strong interaction vertex is treated phenomenologically using an effective Lagrangian [55]. The two standard ways of introducing the pion-nucleon interaction are via the pseudoscalar (PS) or pseudovector (PV) couplings. For elementary fields, without anomalous magnetic interactions, the PS and PV Lagrangians are equivalent, in the lowest order in strong coupling constant. Anomalous magnetic moments of the nucleon are the reason for the breaking for this equivalence, as discussed below. It is well known that the amplitudes derived from the PV coupling are in accord with the low energy theorem (LET) based on gauge invariance and (approximate) chiral symmetry [37]. However, because of the relatively large η mass and big breaking of the chiral SU(3)×SU(3) symmetry [56–59], compared to chiral SU(2)×SU(2) one [60,61], there is no compelling reason to choose the PV form of the ηNN coupling. The Feynman diagram for PV amplitudes are shown in Fig. 1(a)–1(c), where (a) and (b) represent the usual PS amplitudes and (c) is the seagull diagram (proportional to the nucleon anomalous magnetic moment) for the equivalence breaking term, not to be confused with the traditional PV seagull term. Therefore the difference between the PS and the PV coupling at the tree level arises from the fact that the nucleon is a composite particle. Since η is a neutral hadron, the t-channel η exchange and the PV seagull contribution are absent. The effective ηNN interaction Lagrangian can be written as [62]

$$\mathcal{L}_{\eta NN} = g_\eta \left[-i\zeta \bar{N}\gamma_5 N\eta + (1-\zeta)\frac{1}{2M}\bar{N}\gamma_\mu\gamma_5 N\partial^\mu\eta \right], \tag{29}$$

M being the nucleon mass, the two limiting cases being $\zeta = 0$ (PV) and 1 (PS), and the coupling g_η for the ηNN vertex is not very well known [4] and several methods have been used to determine its magnitude. In the SU(3) flavor model, the value of g_{η_8}, where η_8 refers to the pure SU(3) octet η meson, is related to the well-known πNN coupling constant g_π through the relation [4]

$$g_{\eta_8} = \frac{1}{\sqrt{3}}(3 - 4\alpha_p)g_\pi,$$

where $\alpha_p = D/(D+F)$ with D and F being the two type of SU(3) octet meson-baryon couplings. It should be remembered that η_8 does not accurately represent the physical η, which, though predominantly in an SU(3) octet, contains an admixture of the SU(3) singlet configuration. Since the admixture is small [63,64], we shall ignore it to estimate here the g_η, to be taken as g_{η_8}. Val-

ues for α_p range between 0.59 and 0.66 [65,66], which give g_η^2/g_π^2 between 0.043 and 0.14. Other methods of its determination, such as the ratio of the backward angle cross sections of the reactions $\pi^- p \to \eta n$ and $\pi^- p \to \pi^0 n$ (or $K^- p \to \eta\Lambda$ and $K^- p \to \pi^\circ\Lambda$), have given a range of 0.18 to 0.45 for g_η^2/g_π^2 [65]. The η meson coupling has also been determined from fits to low energy nucleon-nucleon [67] scattering in the one boson exchange models, yielding $g_\eta^2/g_\pi^2 \simeq 0.35$. Finally, the $SU(6)_W$ [68] symmetry gives $g_\eta = \sqrt{3}g_\pi/5$, which implies $g_\eta^2/g_\pi^2 = 3/25$, comparable to the SU(3) value given above. Taking $g_\pi^2/4\pi = 13.4$, a conservative range of values for g_η is

$$0.6 \leq g_\eta^2/4\pi \leq 6.4. \tag{30}$$

Thus, the coupling for the ηNN vertex is uncertain, but significantly smaller than the πNN coupling. In our work, the ηNN coupling will be allowed to vary within a range of values bounded by zero and 6.4, unless stated otherwise.

The γNN interaction Lagrangian is well determined within the framework of the quantum electrodynamics (QED):

$$\mathcal{L}_{\gamma NN} = -e\overline{N}\gamma_\mu \frac{(1+\tau_3)}{2} N A^\mu + \frac{e}{4M}\overline{N}(k^s + k^v\tau_3)\sigma_{\mu\nu} N F^{\mu\nu}. \tag{31}$$

$\alpha = e^2/4\pi \simeq 1/137$, N, η, A^μ are the nucleon, η, and photon fields, k^s and k^v are the isoscalar and isovector nucleon anomalous magnetic moments, $k^s = \frac{1}{2}(k_p + k_n)$, $k^v = \frac{1}{2}(k_p - k_n)$, with $k_p = 1.79$ nuclear magnetons (nm) and $k_n = -1.91$ nm, $F^{\mu\nu} = \partial^\nu A^\mu - \partial^\mu A^\nu$. To a first order in e and g_η, the interaction Lagrangians (29) and (31) yield, for the PS coupling ($\zeta = 1$), the nucleon exchange amplitude:

$$i\mathcal{M}_{fi}^{\rm PS} = e g_\eta \bar{U}_f \left[\gamma_5 \frac{\gamma\cdot(p_i+k)+M}{s-M^2}\left(\frac{(1+\tau_3)}{2}\gamma\cdot\varepsilon + \frac{(k^s+k^v\tau_3)}{2M}\gamma\cdot k\gamma\cdot\varepsilon\right) + \left(\frac{(1+\tau_3)}{2}\gamma\cdot\varepsilon + \frac{(k^s+k^v\tau_3)}{2M}\gamma\cdot k\gamma\cdot\varepsilon\right)\frac{\gamma\cdot(p_f-k)+M}{u-M^2}\gamma_5\right] U_i, \tag{32}$$

whereas for the PV case ($\zeta = 0$), γ_5 should be replaced by $\gamma_5\gamma\cdot q$ in the above expression. The first term on the right-hand side of Eq. (32) is because of the s-channel diagram, Fig. 1(a), while the second one corresponds to the u-channel diagram, Fig. 1(b). In the case of a neutron target and the reaction ($\gamma n \to \eta n$), the charge terms proportional to $(1+\tau_3)$ vanish.

An alternative way to introduce PV coupling is to transform the original PS interaction Lagrangian by redefining the nucleon field through the chiral rotation operator $U = \exp(i\frac{g_\eta}{2M}\gamma_5\eta)$ [69]. To first order in g_η in the tree approximation, modifying the nucleon field in the total PS Lagrangian (including the free one) by

$$N \to N + i\frac{g_\eta}{2M}\gamma_5\eta N, \tag{33}$$

leads to

$$\mathcal{L}^{\rm PV} = \mathcal{L}^{\rm PS} + i\frac{e f_\eta}{2M\mu}\bar{N}(k^s+k^v\tau_3)\sigma_{\mu\nu}\gamma_5 N F^{\mu\nu}\eta, \tag{34}$$

where $f_\eta/\mu = g_\eta/(2M)$. The last term on the right-hand side of Eq. (34) is the equivalence breaking term (also known as the "catastrophic" term [69]) and is depicted in Fig. 1(c). Its corresponding amplitude is given by

$$i\mathcal{M}_{fi}^{\rm EB} = \frac{e f_\eta}{M\mu}\bar{U}_f(k^s+k^v\tau_3)\gamma\cdot\varepsilon\gamma\cdot k\gamma_5 U_i. \tag{35}$$

It is straightforward now to determine the A's appearing in Eq. (19),

$$A_1^{\rm PS} = e_N e g_\eta\left[\frac{1}{s-M^2} + \frac{1}{u-M^2}\right], \tag{36}$$

$$A_2^{\rm PS} = 2e_N e g_\eta \frac{1}{(s-M^2)(u-M^2)}, \tag{37}$$

$$A_3^{\rm PS} = -e g_\eta \frac{k_N}{2M}\left[\frac{1}{s-M^2} - \frac{1}{u-M^2}\right], \tag{38}$$

$$A_4^{\rm PS} = -e g_\eta \frac{k_N}{2M}\left[\frac{1}{s-M^2} + \frac{1}{u-M^2}\right], \tag{39}$$

and according to Eq. (34), the PV A's are given by

$$A_1^{\rm PV} = A_1^{\rm PS} + e g_\eta \frac{k_N}{2M^2}, \tag{40}$$

$$A_j^{PV} = A_j^{\rm PS}, \qquad j = 2,3,4, \tag{41}$$

where $e_N = e_p = +1, k_N = k_p$ for protons and $e_N = e_n = 0, k_N = k_n$ for neutrons. The CGLN amplitudes can now be determined using Eq. (28), which lead to the multipoles [given in Eq. (B10)].

There are a few remarks concerning this part of the theory: (1) The nucleon Born terms will project in all the multipoles, including the dominant multipole E_{0+}; (2) the equivalence breaking term contributes only to E_{0+} and M_{1-}, and therefore the difference between the PS and PV couplings would only appear into these multipoles; (3) in our phenomenological fits, the parameter g_η is allowed to vary, while ζ is fixed to either 1 or 0, corresponding to PS or PV cases; and (4) in principle, one should attach form factors at various vertices in Fig. 1(a)–1(b), since the intermediate nucleon is off shell. This, in general, may not preserve gauge invariance [70] and a special procedure needs to be implemented to maintain gauge invariance. Given the poor quality and scarcity of the data, and the general agreement with data, as discussed later, form factors are not introduced at the nucleon vertices.

B. Vector meson exchanges

Though the inclusion of the t-channel exchanges, together with the contributions from other channels may, in general, clash with the ideas of duality [71], their role is unmistakable in the dispersion theory [51]. The role of the t-channel vector meson exchange in neutral pion photoproduction [8,54] is clearly indicated. Thus, they would be included here to see if these contributions influence our ability to extract the nucleon to $N^*(1535)$ electromagnetic amplitude. The strong and electromagnetic vertices involving the vector meson [Fig. 1(d)] are described by the Lagrangians [54]

$$\mathcal{L}_{VNN} = -g_v \overline{N}\gamma_\mu N V^\mu + \frac{g_t}{4M}\overline{N}\sigma_{\mu\nu}N V^{\mu\nu}, \tag{42}$$

$$\mathcal{L}_{V\eta\gamma} = \frac{e\lambda_V}{4\mu}\epsilon_{\mu\nu\lambda\sigma}F^{\mu\nu}V^{\lambda\sigma}\eta, \tag{43}$$

with the vector meson field tensor $V_{\mu\nu} = \partial_\nu V_\mu - \partial_\mu V_\nu$, μ being the η mass. In this energy region, it is enough to consider ρ and ω mesons. The role of ϕ meson is found to be unimportant (less than two percent of the $\rho+\omega$ contribution at threshold), not surprising in the light of the Okubo-Zweig-Iizuka suppression. Exchanges from heavier mesons are expected to be negligible, because of their smaller $\gamma\eta$ decay widths and larger masses. Since the η meson is a neutral particle, in the lowest order, the t-channel η diagonal exchange contribution is zero. Contribution arising from anomalies and connected with the process $\eta \to 2\gamma$, is small and is neglected. Some properties of the vector mesons, pertinent to this work, are summarized in Table I. The vector and tensor couplings (see Table I) of the vector meson-nucleon vertex are taken from analyses of strong interaction processes such as πN and NN scattering using dispersion relations [72,73]. Using the Lagrangian $\mathcal{L}_{V\eta\gamma}$, it is straightforward to calculate the decay width $V \to \gamma\eta$, which is related to the radiative coupling λ_V by

$$\Gamma_{V\to\gamma\eta} = \frac{\alpha(M_V^2-\mu^2)^3}{24\mu^2 M_V^3}\lambda_V^2. \tag{44}$$

From the study of radiative decays [74], extracted parameters, given in Table I, yield

$$\lambda_\rho = 1.06 \pm 0.15, \qquad \lambda_\omega = 0.31 \pm 0.06, \tag{45}$$

in good agreement with quark model calculation [75] which predicts $\lambda_\rho \simeq 3\lambda_\omega$.

The ρ and ω contributions to the amplitude of Fig. 1(d) is

$$i\mathcal{M}_{fi}^{\rho} = -\frac{e\lambda_\rho}{\mu}\frac{i\epsilon_{\mu\nu\alpha\beta}k^\nu q^\alpha \varepsilon^\mu}{t-M_\rho^2} \times \bar{U}_f\tau_3\left\{g_v^\rho\gamma^\beta - \frac{g_t^\rho}{2M}i\sigma^{\beta\delta}(q-k)_\delta\right\}U_i, \tag{46}$$

$$i\mathcal{M}_{fi}^{\omega} = -\frac{e\lambda_\omega}{\mu}\frac{i\epsilon_{\mu\nu\alpha\beta}k^\nu q^\alpha \varepsilon^\mu}{t-M_\omega^2} \times \bar{U}_f\left\{g_v^\omega\gamma^\beta - \frac{g_t^\omega}{2M}i\sigma^{\beta\delta}(q-k)_\delta\right\}U_i. \tag{47}$$

The ρ contributes to the isovector amplitudes, while ω contributes to the isoscalar amplitudes, Eq. (23). Because of near degeneracy of the ρ and ω masses, one can combine their amplitude for the proton target into one effective coupling with the following set of coupling constants:

$$\lambda_\rho g_v^\rho + \lambda_\omega g_v^\omega = 5.93 \pm 0.82, \tag{48}$$

$$\lambda_\rho g_t^\rho + \lambda_\omega g_t^\omega = 17.50 \pm 2.57. \tag{49}$$

We note here a remark made by Bernard *et al.* [61], who point out that the tensor coupling is absent if chiral symmetry is insisted upon. However, in our effective Lagrangian approach, this coupling enters to mimic chiral symmetry violation. This is true also of other effective theories [43].

Expanding the matrix elements in Eqs. (46) and (47) in terms of the invariant amplitudes M_j of Eq. (19) yields

$$A_1^V = \frac{e\lambda_V}{\mu}\frac{g_t^V}{2M}\frac{t}{t-M_V^2}, \tag{50}$$

$$A_2^V = -\frac{e\lambda_V}{\mu}\frac{g_t^V}{2M}\frac{1}{t-M_V^2}, \tag{51}$$

$$A_3^V = 0, \tag{52}$$

$$A_4^V = -\frac{e\lambda_V}{\mu}g_v^V\frac{1}{t-M_V^2}, \tag{53}$$

for the proton target with V being either ρ or ω. For the neutron target the ρ amplitudes are to be multiplied by -1.

An important theoretical issue here is the role of a form factor at the VNN vertex. Brown and co-workers [76] have used a form factor of the type

$$F(t) = \frac{\Lambda^2 - M_V^2}{\Lambda^2 - t}, \tag{54}$$

TABLE I. Coupling constants of vector mesons considered in this work [72–74]. Γ is the full width. The mass of the vector meson is shown in parentheses.

Vector meson	Γ(MeV)	$\Gamma_{V\to\eta\gamma}$(keV)	g_v	g_t
ρ(770 MeV)	153 ± 2	62 ± 17	2.63 ± 0.38	16.05 ± 0.82
ω(782 MeV)	8.5 ± 0.1	6.1 ± 2.5	10.09 ± 0.93	1.42 ± 1.99

preferring a value of $\Lambda^2 \sim 2M_V^2$. The nucleon-nucleon interaction studies [62,67] prefer a value of $\Lambda^2 \simeq 2.0$ GeV^2. Both values are used in this work, and fixed during the fitting procedure. The gauge invariance is preserved, when a form factor is introduced at the VNN vertex, since the photon couples through $F^{\mu\nu}$, as shown in Eq. (43).

C. Nucleon resonance excitation

The s- and u-channel resonance exchanges [Fig. 1(e) and 1(f)] complete the tree-level amplitude for the process (1). Here there are two simplifications. First, since the η meson has zero isospin, only isospin 1/2 nucleon resonances are allowed. Second, below 2 GeV c.m. energy, only two nucleon resonances have significant decay branching ratio into the ηN channel [77–79]: these are the $N^*(1535)$ and $N^*(1710)$ resonances, with the respective ηN branching ratios being 50% and 20–40%. The other three resonances that were considered in this work are $N^*(1440)$, $N^*(1520)$, and $N^*(1650)$. The last two have 0.1% and 1% as respective branching ratios into the ηN channel. The Roper resonance $N^*(1440)$ lies below the ηN threshold of $W = 1487$ MeV and can couple to the η channel only because of its large width. Its ηN coupling is unknown [79]. Since the region around c.m. energy 1535 MeV is the primary interest of this work, other resonances will have small contributions, mainly because they have large masses and small couplings to the ηN channel. Therefore, in the present investigation, the resonances included are $N^*(1440)$, $N^*(1520)$, $N^*(1535)$, $N^*(1650)$, and $N^*(1710)$. A summary of some of the properties of these resonances as given by the Particle Data Group in the 1990 edition [79] is shown in Table II. The more recent values as given in the 1992 edition [79] are also considered here. They are also summarized in Table II. The masses and widths of the resonances considered here are more or less the same in both editions, with the following exceptions: (1) The nominal value of the decay width of $N^*(1440)$ is now 350 MeV; (2) the branching ratio for the process $N^*(1710) \to \eta N$ is not very precisely known: it can vary between 20 to 40%.

1. Spin-1/2 resonances

For a spin-1/2 nucleon resonance the vertex factors are similar to those of the nucleon Born terms discussed earlier. However, it differs at the γNN^* vertex in that the coupling of the type given by the first term on the right-hand side (RHS) of Eq. (31) is absent, since its presence violates gauge invariance, given the inequality of the masses of the N^* and N. Analogous to Eqs. (29) and (31), the spin-1/2 interaction Lagrangians are

$$\mathcal{L}^{\rm PS}_{\eta NR} = -ig_{\eta NR}\bar{N}\Gamma R\eta + \text{H.c.}, \tag{55}$$

$$\mathcal{L}^{\rm PV}_{\eta NR} = \frac{f_{\eta NR}}{\mu}\bar{N}\Gamma_\mu R\partial^\mu\eta + \text{H.c.}, \tag{56}$$

$$\mathcal{L}_{\gamma NR} = \frac{e}{2(M_R+M)}\bar{R}(k_R^s + k_R^v\tau_3)\Gamma_{\mu\nu}NF^{\mu\nu} + \text{H.c.}, \tag{57}$$

where R is the generic notation for the resonance, M_R its mass. The transition magnetic couplings for the proton and neutron targets are respectively $k_R^p = k_R^s + k_R^v$ *and* $k_R^n = k_R^s - k_R^v$. The operator structures for the Γ, Γ_μ, and $\Gamma_{\mu\nu}$ are

$$\Gamma = 1, \quad \Gamma_\mu = \gamma_\mu, \quad \Gamma_{\mu\nu} = \gamma_5\sigma_{\mu\nu}, \tag{58}$$

$$\Gamma = \gamma_5, \quad \Gamma_\mu = \gamma_\mu\gamma_5, \quad \Gamma_{\mu\nu} = \sigma_{\mu\nu}, \tag{59}$$

where (58) and (59) correspond to nucleon resonances of odd and even parities, respectively. Note that differ-

TABLE II. Summary of the properties of the baryon resonances considered in this work. J^π is the spin parity, Γ is the total width. The numbers in parentheses as well as the ones in the last column correspond to the nominal values used by the Particle Data Group [79]. The first row corresponds to PDG 1990 (PDG90) and the second to PDG 1992 (PDG92). We use the notation L_{2I2J} used in πN scattering: the resonance, once produced, decays into πN with a relative orbital angular momentum L, isospin I, and total angular momentum J.

Resonance	J^π	L_{2I2J}	Mass (MeV)	Γ (MeV)	$\Gamma_{N^*\to N\eta}$ (MeV)
$N^*(1440)$	$1/2^+$	P_{11}	1400 – 1480	120 – 350 (200)	Not given
			1430 – 1470	250 – 450 (350)	Not given
$N^*(1520)$	$3/2^-$	D_{13}	1510 – 1530	100 – 140 (125)	~ 0.125
			1515 – 1530	110 – 135 (120)	~ 0.12
$N^*(1535)$	$1/2^-$	S_{11}	1520 – 1560	100 – 250 (150)	67.5 – 82.5
			1520 – 1555	100 – 250 (150)	45 – 75
$N^*(1650)$	$1/2^-$	S_{11}	1620 – 1680	100 – 200 (150)	~ 2.25
			1640 – 1680	145 – 190 (150)	~ 1.5
$N^*(1710)$	$1/2^+$	P_{11}	1680 – 1740	90 – 130 (110)	~ 27.5
			1680 – 1740	50 – 250 (100)	$\sim 20 - 40$

ent parity states are accounted for by inserting γ_5 matrix in the appropriate place. In Eqs. (55) and (56) the ambiguity in the meson-nucleon-resonance coupling calls for the pseudoscalar (PS) or the pseudovector (PV) options. As shown in Sec. III A, the PV coupling could also be introduced through a unitary transformation of the nucleon field [Eq. (33)] to first order in the strong coupling. In the present case one needs to redefine not only the nucleon field but also the resonance field in the total PS Lagrangian ($\mathcal{L}_{\rm free}+\mathcal{L}^{\rm PS}_{\eta NR}+\mathcal{L}_{\gamma NR}$). The appropriate transformations are

$$N\to N+i\frac{g_{\eta NR}}{(M_R\pm M)}\Gamma_{\eta R}, \tag{60}$$

$$R\to R+i\frac{g_{\eta NR}}{(M_R\pm M)}\Gamma_{\eta N}, \tag{61}$$

which give

$$\mathcal{L}^{\rm PV}=\mathcal{L}^{\rm PS}\pm i\frac{ef_{\eta NR}}{(M_R+M)\mu}\bar{N}(k^s_R+k^v_R\tau_3)\sigma_{\mu\nu}\gamma_5 NF^{\mu\nu}\eta, \tag{62}$$

the upper sign corresponding to even parity resonance. Γ is given by Eqs. (58) and (59) and

$$\frac{f_{\eta NR}}{\mu}=\frac{g_{\eta NR}}{(M_R\pm M)}. \tag{63}$$

To first order in $eg_{\eta NR}$, the $\gamma\ N\to\ R\to\ \eta N$ matrix elements for odd parity resonance in the PS coupling are

$$i\mathcal{M}^{{\rm PS},R}_{fi}=\frac{eg_{\eta NR}}{(M+M_R)}\bar{U}_f\{(k^s_R+k^v_R\tau_3)\}\times\left[\frac{\gamma\cdot(p_i+k)+M_R}{s-M_R^2}\gamma_5\gamma\cdot k\gamma\cdot\varepsilon+\gamma_5\gamma\cdot k\gamma\cdot\varepsilon\frac{\gamma\cdot(p_f-k)+M_R}{u-M_R^2}\right]U_i. \tag{64}$$

For the PV case one can either start from the PV Lagrangian or add the equivalence breaking term given by Eq. (35), with the appropriate couplings, to PS matrix elements. The matrix elements of the even parity resonances are deduced from the odd parity ones with the correspondences

$$i\mathcal{M}^R_{fi}(J^\pi=1/2^+)=-i\mathcal{M}^R_{fi}(J^\pi=1/2^-,M_R\to-M_R), \tag{65}$$

leaving the term $(M+M_R)$ in the denominator intact. This can be easily checked by considering the nucleon as the intermediate state and comparing the result with Eq. (32). The amplitudes resulting from the spin-1/2 resonances in the PS coupling are:

$$A^R_1=\pm\frac{eg_{\eta NR}k_R}{(M+M_R)}(M\pm M_R)\left[\frac{1}{s-M_R^2}+\frac{1}{u-M_R^2}\right], \tag{66}$$

$$A^R_2=0, \tag{67}$$

$$A^R_3=\pm\frac{eg_{\eta NR}k_R}{(M+M_R)}\left[\frac{1}{s-M_R^2}-\frac{1}{u-M_R^2}\right], \tag{68}$$

TABLE III. The strong decay widths and the helicity amplitudes as given by the PDG92, compared with the constituent quark model (QM) calculations. For each N^* the first row corresponds to the calculation of Koniuk and Isgur [87], the second row to the calculation of Capstick and Roberts [88].

	$\sqrt{\Gamma_\eta}$ (MeV$^{1/2}$)		$A^p_{1/2}$ (10^{-3} GeV$^{1/2}$)		$A^p_{3/2}$ (10^{-3} GeV$^{1/2}$)	
	PDG	QM	PDG	QM	PDG	QM
$N^*(1440)$	$--$	$+small$	-68 ± 5	-24	$--$	$--$
	$--$	$0.0^{+1.0}_{-0.0}$		4	$--$	$--$
$N^*(1520)$	$+0.35$	$+0.4$	-23 ± 9	-23	$+163\pm8$	$+128$
		$+0.4^{+2.9}_{-0.4}$		-15		$+134$
$N^*(1535)$	$6.7-8.7$	$+5.2$	$+74\pm11$	$+147$	$--$	$--$
		$14.6^{+0.7}_{-1.3}$		76	$--$	$--$
$N^*(1650)$	-1.22	-1.5	$+48\pm16$	$+88$	$--$	$--$
		$-7.8^{+0.1}_{-0.0}$		54	$--$	$--$
$N^*(1710)$	$4.47-6.32$	$+2.9$	$+5\pm16$	-47	$--$	$--$
		5.7 ± 0.3		$+13$	$--$	$--$

$$A_4^R = \pm \frac{e g_{\eta NR} k_R}{(M + M_R)} \left[\frac{1}{s - M_R^2} + \frac{1}{u - M_R^2} \right], \tag{69}$$

with + (−) sign corresponding to negative (positive) excited state and $k_R = k_R^s \pm k_R^v$. The amplitudes due to the PV coupling can be obtained as indicated in Eqs. (40) and (41) with the appropriate coupling.

2. Spin-3/2 resonances

The spin-3/2 excited state involved in this energy region is the odd parity isospin-1/2 $N^*(1520)$ resonance. Even though its ηN coupling (see Tables II, III) is very small, its off-shell effects could be important. We have here important differences with the recent work of Tiator *et al.* [33], who have ignored these effects. We discuss the spin-3/2 propagator problem in Appendix D.

In studying pion-nucleon scattering and pion photoproduction from nucleon at low energies, it is necessary to include, in the theoretical calculations, the contribution of the $\Delta(1232)$ resonance. The question then arises as to how to treat the $\gamma N\Delta$ and $\pi N\Delta$ vertices, which, in the usual approach contain off-shell terms. These interactions have been discussed extensively in the literature [80]. In the present case, the strong and electromagnetic three-point functions are constructed in analogy with those of the $\Delta(1232)$ resonance [8,54,81], apart from taking care of the isospin factors and the odd parity of the $N^*(1520)$. These are

$$\mathcal{L}_{\eta NR} = \frac{f_{\eta NR}}{\mu} \bar{R}^\mu \theta_{\mu\nu}(Z) \gamma_5 N \partial^\nu \eta + \text{H.c.}, \tag{70}$$

$$\mathcal{L}^1_{\gamma NR} = \frac{ie}{2M} \bar{R}^\mu \theta_{\mu\nu}(Y) \gamma_\lambda (k_R^{s\,(1)} + k_R^{v\,(1)} \tau_3) N F^{\lambda\nu} + \text{H.c.}, \tag{71}$$

$$\mathcal{L}^2_{\gamma NR} = -\frac{e}{4M^2} \bar{R}^\mu \theta_{\mu\nu}(X) (k_R^{s\,(2)} + k_R^{v\,(2)} \tau_3) (\partial_\lambda N) F^{\nu\lambda} + \text{H.c.} \tag{72}$$

Here, R^μ is, for example, the $N^*(1520)$ vector spinor, and

$$\theta_{\mu\nu}(V) = g_{\mu\nu} + [\tfrac{1}{2}(1 + 4V)A + V] \gamma_\mu \gamma_\nu, \qquad V = X, Y, Z. \tag{73}$$

Here A is an arbitrary parameter defining the so-called point transformation [see Appendix, Eq. (D4)]. The interaction Lagrangians above have been constructed in such a way that they are invariant under the same point transformation as the free one. The form of $\theta_{\mu\nu}$ gives the most general interaction, limited to the number of derivatives appearing in the Lagrangians in Eqs. (70)–(72) preserving the symmetry of the free Lagrangian. As a result, the physical scattering amplitudes will be independent of A, according to a theorem proved by Kamefuchi, O'Raifeartaigh, and Salam [82]. We choose $A = -1$ for algebraic simplicity. The parameters X, Y, Z, often referred as off-shell parameters, are arbitrary, and will appear in the physical amplitudes. There have been many theoretical attempts [55,83] to fix these parameters but none has been successful. There have also been some claims [83], based on field theoretic arguments originally formulated by Fierz and Pauli [84], that the second coupling term [Eq. (72)] should be absent and a special choice of values for the parameters Z and Y is required. The choice is $Z = \frac{1}{2}, Y = 0, k_R^{(2)} = 0$. One curious consequence of this, arising from the absence of the gauge coupling $k_R^{(2)}$, is that the dynamical freedom of two independent electromagnetic multipoles at the γNN^* vertex is lost. Thus, the magnetic quadrupole ($M2$) to the electric dipole ($E1$) amplitude ratio for the $N^*(1520)$ radiative decay is fixed kinematically, rather than dynamically, yielding the ratio $M2/E1 = (M_R - M)/(3M_R + M) \simeq 11\%$. Available analyses [79] give $31\% \leq M2/E1 \leq 56\%$, inconsistent with $k_R^{(2)} = 0$ for the transition. Similar results would follow for the $\Delta(1232)$ and other spin-3/2 baryons and are discussed in Ref. [80] along with various choices for the off-shell parameters available in the literature. The approach followed by Refs. [8,54] to fit these off-shell parameters to the data will be adopted here.

The scattering amplitudes for the spin-3/2 odd parity resonance excitation in the s channel are

$$i\mathcal{M}_{fi}^{(1),R} = C_1 \bar{U}_f q^\mu \theta_{\mu\nu}(Z) \gamma_5 P^{\nu\lambda}(p) \theta_{\lambda\sigma}(Y) \times (\gamma \cdot \varepsilon k^\sigma - \varepsilon^\sigma \gamma \cdot k) U_i, \tag{74}$$

$$i\mathcal{M}_{fi}^{(2),R} = C_2 \bar{U}_f^\mu \theta_{\mu\nu}(Z) \gamma_5 P^{\nu\lambda}(p) \theta_{\lambda\sigma}(X) \times (p_i \cdot k \varepsilon^\sigma - p_i \cdot \varepsilon k^\sigma) U_i, \tag{75}$$

$$C_1 = -\frac{e k_R^{(1)} f_{\eta NR}}{2M\mu}, \quad C_2 = -\frac{e k_R^{(2)} f_{\eta NR}}{4M^2 \mu},$$

where $k_R^{(i)} = k_R^{s,(i)} \pm k_R^{v,(i)}$, with + (−) corresponding to the proton (neutron) target. As a check, the even parity spin-3/2 exchange [such as $\Delta(1232)$, apart from isospin] scattering amplitudes are obtained by noticing that

$$\gamma_5 P_{\nu\lambda}(p, M_R) = -P_{\nu\lambda}(p, -M_R) \gamma_5. \tag{76}$$

Therefore,

$$i\mathcal{M}_{fi}^{(1),R}(3/2^+) = -i\mathcal{M}_{fi}^{(1),R}(3/2^-, M_R \to -M_R), \tag{77}$$

$$i\mathcal{M}_{fi}^{(2),R}(3/2^+) = i\mathcal{M}_{fi}^{(2),R}(3/2^-, M_R \to -M_R). \tag{78}$$

For the u channel, the strong and electromagnetic vertices need to be interchanged. The expressions for the invariant amplitudes are lengthy and are collected in the Appendix E for convenience.

3. Resonance couplings

The two independent coupling constants of each spin-1/2 resonance can be combined into one effective constant $k_R^p g_{\eta NR}$. The three independent couplings of the spin-3/2 resonance can be grouped into two effective coupling constants $k_R^{p\,(1)} f_{\eta NR}$ and $k_R^{p\,(2)} f_{\eta NR}$, representing the two independent interactions at the electromagnetic

vertex. It is more useful to express these couplings in terms of the experimentally observable quantities such as partial decay widths. For illustration, the dominant resonance $N^*(1535)$ case will be discussed in detail, and a similar procedure can be applied to the remaining resonances.

From the Lagrangian density (57), the S-matrix element for the process $N^*(1535) \to \gamma p$ may be written as

$$S_{fi} = -i\sqrt{\frac{M}{2kE_p}}\frac{\delta^4(p_p + k - p_R)}{(2\pi)^{1/2}}\mathcal{M}_{fi}, \tag{79}$$

where

$$\mathcal{M}_{fi} = \frac{ek_R^p}{(M_R + M)}\bar{U}_p\gamma\cdot k\gamma\cdot\varepsilon\gamma_5 U_R. \tag{80}$$

Here $E_p = \sqrt{M^2 + k^2}$ and k are the energies of the proton and the photon, respectively, defined in the frame where $\mathbf{p}_R = 0$. Upon integrating over the phase space and averaging over the initial spin and summing over the final spins, one obtains the radiative width

$$\Gamma_{N^*(1535)\to\gamma p} = \left(\frac{ek_R^p}{M_R + M}\right)^2 \frac{k^2}{2\pi}\frac{(M_R^2 - M^2)}{M_R}. \tag{81}$$

Alternatively, it may be expressed in terms of the more familiar helicity amplitude $A_{1/2}^p$ [85] through

$$\Gamma_{N^*(1535)\to\gamma p} = \frac{k^2}{\pi}\frac{M}{M_R}|A_{1/2}^p|^2. \tag{82}$$

Comparing the two expressions, one can easily deduce

$$|A_{1/2}^p|^2 = \left(\frac{ek_R^p}{M_R + M}\right)^2 \frac{(M_R^2 - M^2)}{2M}. \tag{83}$$

For the strong coupling, one can use either (55) or (56). The two Lagrangian densities lead to the same result, as they should for an on-shell resonance state. The S-matrix element is

$$S_{fi} = -i\sqrt{\frac{M}{2\omega E_N}}\frac{\delta^4(p_N + q - p_R)}{(2\pi)^{1/2}}\mathcal{M}_{fi}, \tag{84}$$

with

$$\begin{aligned}\mathcal{M}_{fi} &= -i\frac{f_{\eta NR}}{\mu}\bar{U}_N\gamma\cdot qU_R, \\ &= -i\frac{f_{\eta NR}}{\mu}(M_R - M)\bar{U}_N U_R = -ig_{\eta NR}\bar{U}_N U_R.\end{aligned} \tag{85}$$

Here $E_N = \sqrt{M^2 + q^2}$, and ω and q being the energy and momentum of the η meson. The ηN partial decay width is given by

$$\Gamma_{N^*(1535)\to\eta N} = \frac{g_{\eta NR}^2}{4\pi}\frac{q(E_N + M)}{M_R}\bigg|_{W=M_R}. \tag{86}$$

At this stage, it is important to show the relationship between the resonance couplings and the experimentally extracted multipoles or helicity elements describing the process $\gamma + N \to N^* \to \eta + N$. These relations are already known for pion photoproduction. Signs arising from the $N^* \to \pi + N$ decay are involved . Following the prescription given by the Particle Data Group (PDG-76) [79],

$$A_{\ell\pm} = \mp S_X C_{XN}^I A_{1/2}, \tag{87}$$

$$B_{\ell\pm} = \pm S_X\left(\frac{16}{(2J-1)(2J+3)}\right)^{1/2} C_{XN}^I A_{3/2}, \tag{88}$$

$$C_{\ell\pm} = \mp S_X C_{XN}^I S_{1/2}. \tag{89}$$

S_X describes the decay of the resonance into XN, where X is either π or η, and is given by

$$S_X = \left(\frac{1}{(2J+1)\pi}\frac{k_R}{q_R^X}\frac{M}{M_R}\frac{\Gamma_X}{\Gamma^2}\right)^{1/2}. \tag{90}$$

Here k_R, q_R^X are the photon and meson momenta, respectively, in the c.m. frame and evaluated at $W = M_R$ and $k^2 = 0$. C_{XN}^I is a Clebsch-Gordan coefficient related to the isospin coupling in the outgoing channel. As an example, let us consider the amplitudes for the $\pi^0 p$ and ηp production via the $N^*(1535)$ resonance:

$$A_{0+}^{\pi^0 p} = -S_\pi\left(-\sqrt{\frac{1}{3}}\right)A_{1/2} = +\sqrt{\frac{1}{3}}S_\pi A_{1/2}, \tag{91}$$

$$A_{0+}^{\eta p} = -S_\eta A_{1/2}. \tag{92}$$

It is clear that the $A_{0+}^{\pi^0 p}$ has the same sign as $A_{1/2}$ and according to Table III, it is positive, consistent with Walker's analysis [86]. Now, since the relative sign between the π and η strong vertices is positive (see Table III), and the electromagnetic vertices are the same, one then expects that the $A_{0+}^{\eta p}$ is also positive. Therefore, the sign appearing in Eq. (92) is misleading. One has to take into account the isospin convention used and the relative sign between the couplings of $N^* \to \eta N$ and $N^* \to \pi N$. Table III gives the helicity amplitudes and the partial decay width to ηN including the relative sign to πN, as estimated by PDG92 [79], for the resonances considered in this work. The corresponding quantities are also given in the constituent quark model calculations of Koniuk and Isgur [87], as well as Capstick and Roberts [88]. There is agreement in sign between the quark model approaches and the PDG for the $N^*(1520), N^*(1535)$, and $N^*(1650)$ resonances. Being below ηN threshold, the Roper resonance $N^*(1440)$ ηN coupling is not very well determined, but the quark model calculation [88] indicates a small coupling with positive relative sign to the πN coupling. The sign for the $\gamma p \to N^*(1710) \to \eta p$ amplitude is not determined from phenomenological studies [78], but the quark model calculations [88] prefer a negative sign. Therefore, the sign for this amplitude will be allowed to change during the fitting procedure.

4. Approximate unitarization of resonant amplitudes

We now give an approximate unitarization procedure for the resonance excitation amplitudes. We assume a

two-channel K matrix, where the channels are $IN \to N^* \to JN$ with $I, J = \pi, \eta$. This yields, using the PS coupling of meson-nucleon resonance, the expression for the amplitude to excite $N^*(1535)$:

$$E_{0+}^{R,\mathrm{PS}} = -\frac{e g_{\eta NR} k^p}{8\pi W(M_R + M)} \frac{a b_\eta (W - M)(W + M_R)}{W^2 - M_R^2 + i M_R \Gamma_T(W)}, \tag{93}$$

with

$$b_i^2(W) = \frac{(W + M)^2 - m_i^2}{2W}, \quad a^2 = \frac{(W + M)^2}{2W}, \tag{94}$$

$$\Gamma_T(W) = \left(\frac{W + M_R}{2W}\right) \sum_i \left(\frac{b_i^2(W)}{b_i^2(M_R)} \frac{q_i}{q_i^R} \Gamma_i\right), \quad i = \pi, \eta. \tag{95}$$

Γ_i is the partial decay width of S_{11} into (iN), R being S_{11} here, q_i's are the c.m. momenta of the meson i. Again, we have, for S_{11},

$$|g_{\eta NR}| = \left(\frac{4\pi M_R}{q_\eta^R b_\eta^2(M_R)} \Gamma_\eta\right)^{1/2}. \tag{96}$$

Similar expressions for other resonances can be given.

IV. RESULTS AND DISCUSSION

A. Fitting strategy

Previous attempts [26,30,31] at the analysis of η photoproduction data, before the work of Benmerrouche and Mukhopadhyay [13], have not only suffered from the crudeness of the data, but also from *the lack of enough theoretical constraints* in restricting the number of parameters fitted, 24 or more. The effective Lagrangian approach provides us with a tremendous reduction in the number of free parameters, eight in our case. These are g_η, four parameters associated with the spin-1/2 resonances, and three parameters associated with $N^*(1520)$. The resonance masses and widths are taken from analyses of strong interaction processes in order to reduce the number of parameters. Four sets of resonance parameters are used and are given in Table IV. Koch and Cutk parameters are determined through the analyses of πN scattering by Koch [89] and Cutkosky [90], respectively. They differ drastically on the widths of the Roper and $N^*(1535)$ resonances. Bakr parameters are taken from analysis of $\pi^- p \to \eta n$ by Baker *et al.* [78]. Earlier analysis [77] of the same reaction did not include the whole data set; therefore, parameters from Ref. [77] will not be considered here. PDG92 refers to the nominal values estimated by the Particle Data Group in the 1992 edition [79]. The off-shell parameters α, β, δ associated with the spin-3/2 field are not well established theoretically. The parameter α, which appears at the strong interaction vertex, should, in principle, be determined from strong interaction processes such as $\pi^- p \to \eta n$. From pion photoproduction analysis in the $\Delta(1232)$ [8], there is some indication that α should be between zero and two, but all off-shell parameters, in general, are not known. In the present analysis, α will be varied from -1 to 3 and the other two parameters (β, δ) will be determined from the fit to the data. Also, varying the $g_p^{(2)}$ electromagnetic coupling of the D_{13} has not improved the fit considerably and therefore the ratio $g_p^{(2)}/g_p^{(1)}$ is fixed to the PDG value of 0.69. An improved version of the CERN fitter routine, MINUIT is used to minimize the weighted least-squares function χ^2

$$\chi^2 = \sum_i \frac{[X_i - Y_i(a_1, \ldots, a_n)]^2}{\sigma_{X_i}^2}, \tag{97}$$

where X_i represent the experimental observables, σ_{X_i} are their standard deviations, and $Y_i(a_1, \ldots, a_n)$ are the theoretical predictions with a's being the parameters of the theory. In the present case, the observables are the differential cross section and the recoil nucleon polarization, and the summation is over the energies and angles.

TABLE IV. The masses and widths (in MeV) of the baryon resonances considered in this work. Koch and Cutk resonance parameters are determined from $\pi N \to \pi N$ scattering in the analysis by Koch [89] and Cutkosky [90], respectively. Bakr refers to Baker analysis [78] of the data on the reaction $\pi^- p \to \eta n$. PDG92 are the nominal values given by the Particle Data Group (1992).

	Koch	Cutk	Bakr	PDG92
$N^*(1440)$	1410, 135	1440, 340	1472, 113	1440, 350
$N^*(1520)$	1519, 114	1525, 120	1520, 183	1520, 120
$N^*(1535)$	1526, 120	1550, 240	1517, 180	1535, 150
$N^*(1650)$	1670, 180	1650, 150	1670, 200	1650, 150
$N^*(1710)$	1723, 120	1700, 90	1690, 97	1710, 100

B. Analysis of the older data base

The older data base for the differential cross section [14–22] for E_γ between 725 and 1200 MeV contains 137 data points (including the recent measurement by Homma *et al.* [26]). The old polarization measurements [25] (seven data points, of which five are at 90°) for E_γ between 725 and 1100 MeV are also included in the fit. We use this data base to generate the first series of fits, called Fit A. Results of this fit are summarized in Tables V to IX. Note the effect of the off-shell parameter at the strong vertex: for a given set of inputs for resonances, the effect of this parameter is not large. There is also

some influence of the vector meson form factor through its cutoff parameter on the fitted results.

Below we discuss in detail our analysis of the old data base. Our comments on the new data will supplement these observations.

1. *Resonance characteristics*

In Tables V to XI, all but the last two relevant to the old data base, the resonances have been renamed for brevity: for example, S_1 denotes the $N^*(1535)$, P_1 the Roper resonance, etc. The total χ^2 is given separately for the differential cross section (XS) and the recoil nucleon polarization (pol). The total χ^2 per degree of freedom is denoted by $\chi^2_{\rm TOT}/N_{\rm DF}$. $\sqrt{\Gamma_\eta}A_{1/2,3/2}$ has been multiplied by 1000 and the helicity amplitudes $A_{1/2,3/2}$ are expressed in the standard units of 10^{-3} GeV$^{-1/2}$. As there are large differences in the masses and widths of the resonances in various analyses, we have investigated here how the results of our fitting are affected by a particular choice of those parameters. One important finding is that the quantity ξ, characteristic of the photoexcitation of the $N^*(1535)$ resonance and its decay into the η-nucleon channel, defined as

$$\xi = \sqrt{\chi' \Gamma_\eta}\, A_{1/2}/\Gamma_T, \tag{98}$$

where $\chi' = Mk/qM_R$, k and q to be evaluated at $W = M_R$, *is not* sensitive to uncertainties of the resonance parameters and other details of the effective Lagrangian approach. Taking a simple average over the new results from PDG92 fits gives a rather precise determination of ξ [91]:

$$\xi = (2.2 \pm 0.2) \times 10^{-1}\ \text{GeV}^{-1}. \tag{99}$$

This quantity should be of fundamental interest to a precision test of hadron models. Another important feature of this analysis is that the product $[\sqrt{\Gamma_\eta}A_{1/2}]_{S1}$ extracted from the data does not depend on the details

TABLE V. Couplings obtained by fitting the old data base for η photoproduction, using different sets of masses and widths of the resonances. The cutoff used for the vector meson form factor [Eq. (60)] is indicated by Λ^2. The off-shell parameter at the strong vertex is fixed to $\alpha = -1$. There are 137 differential cross sections and seven polarization data points below $E_\gamma = 1.2$ GeV in the old base. Eight parameters are fitted. The ηNN and ηNN^* couplings are pseudoscalar. The corresponding helicity amplitudes are listed in units of 10^{-3} GeV$^{1/2}$. The quantity ξ characteristic of the photoexcitation of the dominant resonance $N^*(1535)$ and its decay into the ηN channel is also given in units 10^{-4} MeV^{-1}.

	PDG92		Koch		Bakr	
Λ^2(GeV^2)	2.0	1.2	2.0	1.2	2.0	1.2
g_η	2.6	4.1	6.8	5.8	4.2	4.1
$[\sqrt{\Gamma_\eta}A_{1/2}]_{S1}$	26.6	26.2	20.0	20.3	26.7	26.3
$[A_{1/2}]_{S1}$	97.0	95.6	81.7	82.9	104.9	103.3
$[\sqrt{\Gamma_\eta}A_{1/2}]_{S2}$	−6.9	−7.0	−3.8	−4.1	−17.3	−14.3
$[A_{1/2}]_{S2}$	179.4	180.9	72.4	78.5	315.4	260.8
$[\sqrt{\Gamma_\eta}A_{1/2}]_{P1}$	−3.8	−0.08	0.03	0.03	−0.1	−0.2
$[A_{1/2}]_{P1}$	−17.4	−0.4	0.1	0.1	−1.6	−2.6
$[\sqrt{\Gamma_\eta}A_{1/2}]_{P2}$	3.9	2.9	4.1	5.0	4.3	3.4
$[A_{1/2}]_{P2}$	22.7	16.7	23.7	28.9	27.6	22.0
$[\sqrt{\Gamma_\eta}A_{1/2}]_{D1}$	−0.1	−0.1	−0.2	−0.2	−0.07	−0.09
$[A_{1/2}]_{D1}$	−9.5	−9.3	−15.2	−16.9	−5.3	−6.5
$[\sqrt{\Gamma_\eta}A_{3/2}]_{D1}$	0.8	0.8	1.2	1.4	0.5	0.7
$[A_{3/2}]_{D1}$	72.4	70.4	116.1	128.9	40.3	49.3
β	1.4	0.9	1.0	1.0	1.1	0.8
δ	1.4	1.0	1.4	1.3	1.4	1.3
χ^2(XS)	239.8	226.9	295.0	266.5	259.8	242.1
χ^2(pol)	30.5	12.2	12.1	13.8	29.6	16.6
$\chi^2_{\rm tot}/N_{\rm DF}$	2.0	1.8	2.3	2.1	2.1	1.9
ξ	2.22 ± 0.15	2.19 ± 0.15	2.19 ± 0.18	2.23 ± 0.17	2.07 ± 0.14	2.04 ± 0.14

TABLE VI. Same as Table V, with $\alpha = 1$.

	PDG92		Koch		Bakr	
$\Lambda^2(\mathrm{GeV}^2)$	2.0	1.2	2.0	1.2	2.0	1.2
g_η	5.8	4.1	6.3	5.1	6.1	4.1
$[\sqrt{\Gamma_\eta} A_{1/2}]_{S1}$	25.8	26.1	20.2	20.8	26.0	26.6
$[A_{1/2}]_{S1}$	94.1	95.5	82.5	84.9	102.0	104.5
$[\sqrt{\Gamma_\eta} A_{1/2}]_{S2}$	−6.1	−7.0	−5.5	−6.7	−13.3	−15.1
$[A_{1/2}]_{S2}$	156.7	180.3	105.9	128.9	243.0	275.7
$[\sqrt{\Gamma_\eta} A_{1/2}]_{P1}$	−1.4	−1.4	−2.3	0.03	−0.06	−0.3
$[A_{1/2}]_{P1}$	−6.2	−6.4	−7.4	0.1	−0.7	−3.6
$[\sqrt{\Gamma_\eta} A_{1/2}]_{P2}$	3.8	3.9	7.7	7.1	3.3	3.4
$[A_{1/2}]_{P2}$	22.2	22.6	44.4	41.0	21.4	21.9
$[\sqrt{\Gamma_\eta} A_{1/2}]_{D1}$	−0.2	−0.2	−0.3	−0.2	−0.2	−0.2
$[A_{1/2}]_{D1}$	−17.6	−14.8	−24.2	−20.4	−14.1	−11.7
$[\sqrt{\Gamma_\eta} A_{3/2}]_{D1}$	1.5	1.2	2.0	1.7	1.4	1.2
$[A_{3/2}]_{D1}$	133.6	112.6	184.8	155.6	106.7	89.2
β	−0.3	0.09	−0.3	−0.06	−0.3	0.2
δ	−3.0	−1.5	−4.0	−2.6	−1.5	0.8
$\chi^2(\mathrm{XS})$	229.2	221.0	254.7	258.4	244.0	235.7
$\chi^2(\mathrm{pol})$	14.4	12.5	16.2	17.3	15.6	13.7
$\chi^2_{\mathrm{tot}}/N_{\mathrm{DF}}$	1.8	1.7	2.0	2.0	1.9	1.8
ξ	2.16 ± 0.15	2.19 ± 0.15	2.22 ± 0.18	2.28 ± 0.17	2.02 ± 0.14	2.07 ± 0.14

of the background (given a set of resonances). Given a particular choice of resonance parameters, indicated in parentheses, we find the following parameters for the $N^*(1535)$, using the old data base:

$$M_R(\mathrm{MeV}), \Gamma_T(\mathrm{MeV}) A_{1/2}(10^{-3}\ \mathrm{GeV}^{-1/2})$$

$$1535, 150\ (\mathrm{PDG92}) \qquad 97 \pm 7\ , \tag{100}$$

$$1526, 120\ (\mathrm{Koch}) \qquad 87 \pm 6\ , \tag{101}$$

$$1517, 180\ (\mathrm{Bakr}) \qquad 104 \pm 6\ , \tag{102}$$

$$1550, 240\ (\mathrm{Cutk}) \qquad 173 \pm 9\ . \tag{103}$$

Here the agreement between the first three sets of numbers is reasonable, while the figures for the Cutk do not agree with the previous ones. Given the large difference in the total width for the $N^*(1535)$ between the Cutk set and the others, this is not surprising. However, the fit with Bakr falls short of the experimental data (Figs. 4 and 5). This may be due to the unusually low value of the ηN branching ratio (36%). We refer the reader to a recent analysis by Manley and Saleski [92], who have extracted resonance parameters using the isobar model to analyze the data for the $\pi N \to \pi\pi N$. Their inferred mass and width of the $N^*(1535)$ agree well with the PDG92 nominal values.

We thus obtain, from the old data base, and using inputs from the PDG92,

$$A_{1/2} = (97 \pm 7) \times 10^{-3}\ \mathrm{GeV}^{-1/2}, \tag{104}$$

for the proton. This lies in between the predicted extremes of recent theoretical estimates in the quark model [87,93–95] ranging from 54 to 162, in the same units. The latest of these is from Capstick [88], who has obtained a value $A_{1/2} = 76 \times 10^{-3}\ \mathrm{GeV}^{-1/2}$. The corresponding value, reported by the PDG92, extracted from the pion photoproduction data is 74 ± 11 [79]. The origin of the disagreement between the resonant amplitudes extracted from η and pion photoproduction data is not understood at present. The quark model estimates are still too crude to be definitive in testing the model. The issues of the truncation of the model space and the lack of current conservation [96] are just some of many unresolved issues. Much work remains to be done here.

As far as the helicity amplitudes of the other resonances are concerned, the old data set does not permit an accurate extraction, except to allow the conclusion that they are consistent, in general, with the results extracted from pion photoproduction analyses. The results obtained for each resonance will now be briefly discussed.

(1) Assuming a branching ratio to ηN of 1%, the $N^*(1650)$ photocoupling can be as large as four times that obtained by pion photoproduction analysis and by the quark model calculations. This might be because of

TABLE VII. Results of fitting the old data base using the pseudovector ηNN coupling, with the pseudoscalar ηNN^* couplings. Only the values of α that give the lowest $\chi^2/N_{\rm DF}$ are shown. In the fit, the value of α is fixed. Other notations are the same as in Table V.

	PDG92		Koch		Bakr	
Λ^2(GeV^2)	1.2	2.0	1.2	2.0	1.2	2.0
g_η	4.4	3.4	5.0	6.2	4.3	4.6
$[\sqrt{\Gamma_\eta}A_{1/2}]_{S1}$	26.1	26.6	20.5	20.1	26.5	26.6
$[A_{1/2}]_{S1}$	95.2	97.0	83.6	81.9	104.1	104.4
$[\sqrt{\Gamma_\eta}A_{1/2}]_{S2}$	−7.0	−7.2	−6.5	−5.6	−14.9	−13.9
$[A_{1/2}]_{S2}$	181.5	185.5	125.3	107.0	271.9	254.2
$[\sqrt{\Gamma_\eta}A_{1/2}]_{P1}$	−1.8	−2.0	−3.4	−4.3	−0.3	−0.3
$[A_{1/2}]_{P1}$	−8.4	−9.2	−10.8	−13.6	−3.2	−3.2
$[\sqrt{\Gamma_\eta}A_{1/2}]_{P2}$	3.8	3.1	8.0	7.9	3.3	3.0
$[A_{1/2}]_{P2}$	21.9	17.9	46.4	45.7	21.5	19.4
$[\sqrt{\Gamma_\eta}A_{1/2}]_{D1}$	−0.1	−0.2	−0.2	−0.2	−0.1	−0.2
$[A_{1/2}]_{D1}$	−11.9	−18.3	−19.1	−19.0	−8.4	−18.2
$[\sqrt{\Gamma_\eta}A_{3/2}]_{D1}$	1.0	1.5	1.6	1.5	0.9	1.9
$[A_{3/2}]_{D1}$	90.5	138.6	146.1	145.1	64.1	138.5
α	1.0	0.0	1.0	1.0	1.0	0.0
β	0.9	1.3	0.5	0.4	1.2	1.2
δ	−10.2	0.04	−9.4	−12.6	−8.7	0.07
χ^2(XS)	224.2	230.1	255.6	268.9	240.7	236.0
χ^2(pol)	13.3	11.3	17.5	19.2	15.8	12.0
$\chi^2_{\rm tot}/N_{\rm DF}$	1.8	1.8	2.0	2.1	1.9	1.8
ξ	2.18 ± 0.15	2.22 ± 0.15	2.25 ± 0.18	2.20 ± 0.18	2.06 ± 0.14	2.06 ± 0.14

the ambiguity in determining the ηN branching ratio.

(2) The $N^*(1440)$ coupling is found to be very small indicating that this resonance may not be a significant player in the (γ,η) process. Recently, there have been some speculation [97] that the $N^*(1440)$ might be a candidate for the lightest hybrid state, consisting of three valence quarks and one valence gluon. A precise determination of the $N^*(1440)$ photocoupling can provide a powerful tool to distinguish between different internal structures for this hadron: q^3 and q^3G, where q is a valence quark and G is a valence gluon.

(3) The $N^*(1520)$ off-shell contribution is found to be very important and correlates with the nucleon and the vector meson contributions. However, this is not so in the case of Cutk, as can be seen by comparing columns 3 and 5 of Table VIII and Table IX. This conclusion may be connected with the relatively large width of the $N^*(1535)$ in the Cutk set. The off-shell parameters depend on the cutoff in the vector meson form factor and the choice of coupling for the ηNN vertex (compare, for example, Tables VI and VII). The photocouplings of the $N^*(1520)$ are consistent with pion photoproduction studies.

(4) The $N^*(1710)$ is poorly determined from the $\gamma N \to \pi N$ reactions. *This resonance photocoupling could be well determined from the present analysis if there were enough data around* $W \simeq 1710$ GeV. All it can be said is that our fits favor a positive sign for the product $[\sqrt{\Gamma_\eta}A_{1/2}]_{P2}$, in *disagreement* with the quark model prediction of Koniuk and Isgur but *in agreement* with the Capstick and Roberts' results (see Table III).

2. *Measured quantities in the experiments on η photoproduction*

a. Differential cross section. In general, reasonable fits to the available data on differential cross section are obtained. The best fit to the data is obtained with the PDG parameters. Sample fits using PDG, Koch, and Bakr resonance parameters are displayed in Figs. 2–4 for the c.m. angle of 90°. The s-channel excitation of the $N^*(1535)$ resonance dominates the differential cross section, while the u-channel contribution is found to be negligible. The three sets are in good agreement with the data, but start deviating from each other above $E_\gamma =$ 1100 MeV. Around this energy region, the $N^*(1710)$ is the dominant resonance contribution because of its large ηN branching ratio.

TABLE VIII. Fitted couplings from the old data base using Cutkosky (Cutk) resonance parameters. The ηNN^* coupling is pseudoscalar, while ηNN coupling chosen is shown. Only lowest $\chi^2/N_{\rm DF}$ are given.

$\Lambda^2(\mathrm{GeV}^2)$	2.0	1.2	1.2	1.2
ηNN	PS	PS	PV	PS
g_η	0.06	2.0	0.9	1.7
$[\sqrt{\Gamma_\eta}A_{1/2}]_{S1}$	45.0	44.2	44.7	44.2
$[A_{1/2}]_{S1}$	176.7	173.6	175.7	173.7
$[\sqrt{\Gamma_\eta}A_{1/2}]_{S2}$	−13.1	−11.0	−12.8	−11.2
$[A_{1/2}]_{S2}$	277.0	232.4	269.0	235.5
$[\sqrt{\Gamma_\eta}A_{1/2}]_{P1}$	−2.4	−1.9	−1.3	−3.1
$[A_{1/2}]_{P1}$	−10.9	−8.6	−6.0	−14.3
$[\sqrt{\Gamma_\eta}A_{1/2}]_{P2}$	1.8	0.6	1.7	0.9
$[A_{1/2}]_{P2}$	12.2	4.3	11.3	5.9
$[\sqrt{\Gamma_\eta}A_{1/2}]_{D1}$	−0.07	−0.04	−0.07	−0.008
$[A_{1/2}]_{D1}$	−6.0	−3.5	−6.8	−0.8
$[\sqrt{\Gamma_\eta}A_{3/2}]_{D1}$	0.5	0.3	0.6	0.06
$[A_{3/2}]_{D1}$	44.5	26.0	50.5	5.6
α	2.0	1.0	2.0	0.0
β	−0.04	−0.09	0.6	0.2
δ	5.1	9.9	3.8	9.9
χ^2(XS)	217.3	220.1	214.9	225.6
χ^2(pol)	11.8	11.6	11.5	11.6
$\chi^2_{\rm tot}/N_{\rm DF}$	1.7	1.7	1.7	1.8
ξ	2.21 ± 0.11	2.17 ± 0.12	2.20 ± 0.11	2.17 ± 0.12

b. Total cross section. The old data base on the total cross section [24] suffers from poor photon energy resolution and counting statistics, and thus limits the quality of physics extractable from them. The model prediction is in agreement with the data for the three sets of resonance parameters as displayed in Fig. 5. There is one data point well outside our fit. The Bakr parameters tend to underestimate the total cross section.

c. Polarization observables. Our predictions for polarized target asymmetry and photon asymmetry are also shown. All three sets show more or less the same behavior for the polarization observables below the photon lab energy of one GeV, but yield very different predictions above this energy level. Therefore, polarization observables should provide a more stringent test of the model. The meager data on the recoil nucleon polarization are too poor to be of any quantitative value.

C. Analysis of the Bates angular distribution data

The recent η photoproduction experiment at the Bates Laboratory by the Pittsburgh-Boston-LANL Collaboration [27] will now be discussed. This group has been able to measure the angular distribution for (γ, η) reaction at photon lab energies of 729 and 753 MeV at six angles. These data are more or less flat as a function of angle (Fig. 6) at $E_\gamma = 729$ MeV, consistent with the predictions of our effective Lagrangian approach, using the parameters of the Fit A. However, the data set at $E_\gamma = 753$ MeV exhibit a deviation from isotropy, in disagreement with the prediction of the Fit A (Fig. 6). This suggests some *inconsistency* between the new Bates data and the old data set from which the Fit A has been derived.

We now use the older data set and the Bates data together for a global fit, Fit B. The resultant resonance parameters are shown in Table X. This is a compromise fit between two somewhat incompatible data sets.

Finally, we can, of course, use the Bates data alone and try to fit the effective Lagrangian parameters. In doing so, we shall keep the $N^*(1535)$, $N^*(1650)$, and $N^*(1710)$ parameters fixed at the fit B level, along with the ηNN coupling constant, as this data set, by itself, cannot yield informations on the properties of all of these resonances, because of the limited energy coverage. Instead, we use this data set to explore the nature of coupling of the nucleon Born terms and the properties of the $N^*(1440)$ and $N^*(1520)$ resonances. These fits, called Fit C, are shown in Fig. 7. The resultant fit still shows dominance

TABLE IX. Fitted parameters using the old data base and the PV coupling at the ηNN and ηNN^* vertices. The cutoff for the vector meson form factor is fixed at 1.2 GeV^2.

	PDG92	Koch	Bakr	Cutk
g_η	3.7	5.3	4.4	2.2
$[\sqrt{\Gamma_\eta}A_{1/2}]_{S1}$	26.0	20.1	25.5	43.3
$[A_{1/2}]_{S1}$	95.0	82.2	100.2	169.9
$[\sqrt{\Gamma_\eta}A_{1/2}]_{S2}$	−9.1	−6.4	−14.6	−11.8
$[A_{1/2}]_{S2}$	234.7	122.7	265.7	248.6
$[\sqrt{\Gamma_\eta}A_{1/2}]_{P1}$	−0.4	−2.3	−0.2	−2.2
$[A_{1/2}]_{P1}$	−1.7	−7.4	−2.3	−10.0
$[\sqrt{\Gamma_\eta}A_{1/2}]_{P2}$	2.0	7.7	3.0	0.7
$[A_{1/2}]_{P2}$	11.7	44.4	19.2	4.4
$[\sqrt{\Gamma_\eta}A_{1/2}]_{D1}$	−0.04	−0.2	−0.1	−0.007
$[A_{1/2}]_{D1}$	−3.8	−19.1	−8.6	−0.6
$[\sqrt{\Gamma_\eta}A_{3/2}]_{D1}$	0.3	1.6	0.9	0.05
$[A_{3/2}]_{D1}$	28.8	145.9	65.6	4.5
α	1.0	1.0	1.0	1.0
β	2.5	0.4	0.9	4.7
δ	−12.9	−8.6	−6.0	4.2
χ^2(XS)	228.2	247.3	232.6	229.0
χ^2(pol)	14.2	16.0	14.2	11.5
$\chi^2_{\rm tot}/N_{\rm DF}$	1.8	2.0	1.8	1.8
ξ	2.18 ± 0.14	2.21 ± 0.15	1.98 ± 0.12	2.13 ± 0.11

of the $N^*(1535)$ in the differential cross section. The parameters for the resonances change somewhat (Table XI), compared with what we have obtained from the old data base. As discussed below in Sec. IV E, *the E_{0+} amplitude, extracted from the Bates data, is not in agreement with those from the other data sets.*

D. A look at the preliminary Mainz data

The results of an exhaustive η photoproduction experiment [29] from the Mainz Microtron are available in a preliminary form, following their presentations at the Trieste, Perugia, and Dubna conferences [29]. We emphasize the word *preliminary*, as these data are yet to be published in a definitive form. The data, presented so far, are the angular distributions at the photon laboratory energies of E_γ = 722.5, 737.5, 752.5, 767.5, and 782.5 MeV, though the absolute normalizations of these distributions are yet to be determined. Also available from the recent Dubna conference are the preliminary Mainz data on the total η photoproduction cross section, again with the absolute normalization being arbitrary. We compare them with our predictions from the effective Lagrangian approach, with parameters determined from the old world supply of data, Fit A. The *shapes* of both the angular distributions and total cross section of the Mainz data are predicted rather nicely. The arbitrary factor needed to bring the data of the differential and total cross section is the same. We are waiting with anticipation for the definitive normalizations of these data.

We can get an idea of the importance of the preliminary Mainz data on the physics of the N^* resonances, particularly $N^*(1535)$. The parameter ξ, in units of 10^{-1} GeV^{-1}, defined earlier, extracted only from the Mainz data (Fit D) is

$$\xi = 2.0 \pm 0.1, \tag{105}$$

for the off-shell parameter $\alpha = -1$, and

$$\xi = 2.3 \pm 0.1, \tag{106}$$

for the off-shell parameter $\alpha = +1$, for the vector meson form factor cutoff parameter $\Lambda^2 = 1.2$ GeV^2. These compare with the value

$$\xi = 2.2 \pm 0.2 \tag{107}$$

from our Fit A of the world's old data set. Thus, the error

TABLE X. Fitting the old data base together with the new Bates data [28].

Λ^2	2.0	1.2	2.0	1.2
g_η	5.9	4.6	5.9	4.3
$[\sqrt{\Gamma_\eta}A_{1/2}]_{S1}$	26.2	26.3	26.2	26.4
$[A_{1/2}]_{S1}$	95.5	96.0	95.8	96.2
$[\sqrt{\Gamma_\eta}A_{1/2}]_{S2}$	−5.5	−6.8	−6.4	−7.4
$[A_{1/2}]_{S2}$	142.9	176.7	164.6	192.2
$[\sqrt{\Gamma_\eta}A_{1/2}]_{P1}$	0.7	1.1	0.5	0.2
$[A_{1/2}]_{P1}$	3.3	4.9	2.5	1.1
$[\sqrt{\Gamma_\eta}A_{1/2}]_{P2}$	2.1	2.8	3.1	3.6
$[A_{1/2}]_{P2}$	12.1	16.4	18.1	20.7
$[\sqrt{\Gamma_\eta}A_{1/2}]_{D1}$	−0.09	−0.1	−0.2	−0.2
$[A_{1/2}]_{D1}$	−8.5	−9.6	−15.4	−13.7
$[\sqrt{\Gamma_\eta}A_{3/2}]_{D1}$	0.7	0.8	1.3	1.1
$[A_{3/2}]_{D1}$	64.8	72.6	116.5	104.2
α	−1.0	−1.0	1.0	1.0
β	1.1	0.9	−0.3	0.1
δ	1.7	1.1	−2.7	−1.3
χ^2(XS)	310.5	284.7	287.4	281.6
χ^2(pol)	13.2	13.2	14.5	13.2
$\chi^2_{\rm tot}/N_{\rm DF}$	2.2	2.0	2.1	2.0
ξ	2.19 ± 0.15	2.20 ± 0.14	2.20 ± 0.15	2.21 ± 0.14

on the ξ parameter is somewhat reduced, using the Mainz data. Taking $\Gamma_\eta = 75$ MeV, the preliminary Mainz data yield a value of $A_{1/2}$, in units of 10^{-3} GeV$^{-1/2}$,

$$A_{1/2} = 88, 101, \tag{108}$$

for the above two cases, consistent with our results from the older data set, Eq. (100). It is substantially larger than the latest results from the quark model [88] 75×10^{-3} GeV$^{-1/2}$, and that from the analysis of pion photoproduction. The results [Eqs. (105), (106), and (108)] are subject to revision, if the Mainz data change substantially, as they are reanalyzed, but the basic conclusion of their importance in determining the ξ parameter should remain valid. For comparison, we quote here the values of ξ and $A_{1/2}$ extracted from the Bates data under similar theoretical assumptions in analysis:

$$\xi = 2.1 \pm 0.1, 1.8 \pm 0.3,$$
$$A_{1/2} = 91, \quad 78. \tag{109}$$

E. The E_{0+} amplitude at threshold

The threshold η photoproduction and its impact on the determination of the ηNN coupling constant is the last topic we wish to address here. It is particularly interesting to contrast the E_{0+} amplitude for the η photoproduction with that for the π^0 photoproduction at their respective thresholds. Table XII demonstrates the real part of the E_{0+} amplitude for the η photoproduction off the proton at threshold, contrasted with the same for the π^0 photoproduction. While there is a clear preference for the PV coupling at the $\pi^0 NN$ vertex, this is not so for the η meson, as we have pointed out earlier. Here, we have given the E_{0+} amplitude as determined from the Fits A, B, C, and D, demonstrating the relevance of different data sets in the context of the E_{0+} amplitude. *All fits agree in the dominant role of the $N^*(1535)$ resonance.*

Interestingly, the value of the ηNN coupling constant extracted from the fits is only mildly sensitive to the choice of the PV or PS coupling at the meson-nucleon vertex. From fits to all data sets, using the resonance parameter set of PDG92, we get

$$0.2 \leq g_\eta \leq 6.2. \tag{110}$$

For the η photoproduction, the vector meson contributions are sizable, but the $N^*(1535)$ excitation amplitude in the s channel stands out, in contrast with the π^0 case, where both the vector meson and the $\Delta(1232)$ contributions are minor. Another important contribution to η photoproduction is from the $N^*(1520)$, with its off-shell

TABLE XI. Fits using the Bates data [28] only.

Λ^2	2.0	1.2	2.0	1.2
g_η	5.9	4.6	5.9	4.3
$[\sqrt{\Gamma_\eta}A_{1/2}]_{S1}$	26.2	26.3	26.2	26.4
$[A_{1/2}]_{S1}$	95.5	96.0	95.8	96.2
$[\sqrt{\Gamma_\eta}A_{1/2}]_{S2}$	−5.5	−6.8	−6.4	−7.4
$[A_{1/2}]_{S2}$	142.9	176.7	164.6	192.2
$[\sqrt{\Gamma_\eta}A_{1/2}]_{P1}$	0.02	0.02	0.02	−0.8
$[A_{1/2}]_{P1}$	0.1	0.1	0.1	−3.7
$[\sqrt{\Gamma_\eta}A_{1/2}]_{P2}$	2.1	2.8	3.1	3.6
$[A_{1/2}]_{P2}$	12.1	16.4	18.1	20.7
$[\sqrt{\Gamma_\eta}A_{1/2}]_{D1}$	−0.5	−0.5	−0.1	−0.1
$[A_{1/2}]_{D1}$	−46.8	−46.5	−9.6	−9.8
$[\sqrt{\Gamma_\eta}A_{3/2}]_{D1}$	3.9	3.9	0.8	0.8
$[A_{3/2}]_{D1}$	355.4	353.3	72.9	74.0
α	−1.0	−1.0	1.0	1.0
β	0.7	0.7	8.2	8.6
δ	−0.3	−0.4	10.0	10.0
χ^2(XS)	4.8	4.7	5.7	5.8
$\chi^2_{\rm tot}/N_{\rm DF}$	0.6	0.6	0.7	0.7
ξ	2.19	2.20	2.20	2.21

TABLE XII. Contributions to the real part of the E_{0+} multipole, in units of $10^{-3}/m_{\pi+}$, for the η and π^0 photoproduction at their respective thresholds. For all fits, $\alpha = +1$ and $\Lambda^2 = 1.2$ GeV^2 are used. Fits A, B, C, and D are defined in the text, based on different combinations of data bases.

Contributions	Fit A	Fit B	Fit C	Fit D	π^0
Nucleon Born terms	−6.05	−6.37	−6.37	−3.47	−2.46
$\rho + \omega$	2.89	2.89	2.89	2.89	0.04
$\Delta(1232)$	−−	−−	−−	−−	0.35
$N^*(1535)$	12.06	12.16	12.16	12.16	0.03
$N^*(1440)$	−0.47	0.08	−0.27	−1.22	0.01
$N^*(1650)$	−0.94	−1.00	−1.00	−1.00	0.01
$N^*(1520)$	1.46	1.39	−6.08	0.43	0.08
$N^*(1710)$	0.25	0.23	0.23	0.23	0.00
Total	9.21	9.39	1.56	10.02	−1.94
Experiment	−−	−−	−−	−−	-2.0 ± 0.2 [a]

[a]The reanalysis [44,45] of the near threshold experiment [35] on π^0 photoproduction on the proton.

effects tending to interfere destructively with the large contribution of the PS Born terms, or constructively with the smaller contribution of the PV Born terms.

V. CONCLUSIONS

Given the renewed theoretical interest arising from the prospect of testing QCD in the nonperturbative domain by computing hadron properties, and the experimental possibilities of exploring many of these properties in the novel electron and/or photon facilities now under development, particularly CEBAF, η photoproduction on the proton has been investigated in the $N^*(1535)$ resonance region, with a view to help understand the structure of the nucleon and its excited states. In this paper, the goal has been to extract the product of the electric dipole transition amplitude $\gamma p \to N^*(1535)$ and the decay amplitude $N^*(1535) \to \eta p$, from the existing old experiments and new ones. The dominant tree-level contributions considered here have been computed in the framework of the effective Lagrangian formalism, proven to be very successful in describing pion photoproduction in the $\Delta(1232)$ region. Unlike the π° case, there is no compelling reason to choose the pseudovector (PV) form of the ηNN (or ηNN^*) coupling, and we have investigated both the PV and the pseudoscalar (PS) couplings at the ηNN and the ηNN^* vertices. We have taken into account various background contributions, and have attempted to extract information on the excitation and decay of the $N^*(1535)$ resonance. Our conclusions are as follows.

(1) Unlike the pion, where there is a clear preference for the PV coupling at the meson-nucleon vertex, seen in the threshold π^0 photoproduction data on the proton, the present experimental data on η photoproduction do not distinguish between pseudovector and pseudoscalar couplings, as contributions from various resonances and nonresonant background compensate. This is not surprising, as the chiral symmetry is strongly broken by the η mass. Likewise, there is no strong preference for either coupling at the ηNN^* vertices.

(2) The extracted amplitude shows that the π^0 and the η photoproduction processes near threshold have very significant differences, even as they share the common contributions, such as the nucleon Born terms, the basis for the predictions of the low energy theorems (LET's) for the pion case. Among these differences, the contribution to the η photoproduction by the s-channel excitation of the $N^*(1535)$ resonance is obvious. The situation is quite different in the π^0 case, where one probes only the nucleon Born terms, and, through it, the chiral symmetry [58,103] breaking effects, with minor contributions from the $\Delta(1232)$ excitation. Thus, the chiral symmetry breaking effects are hard to quantify in the η case.

(3) Many previous attempts at the analysis of η pho-

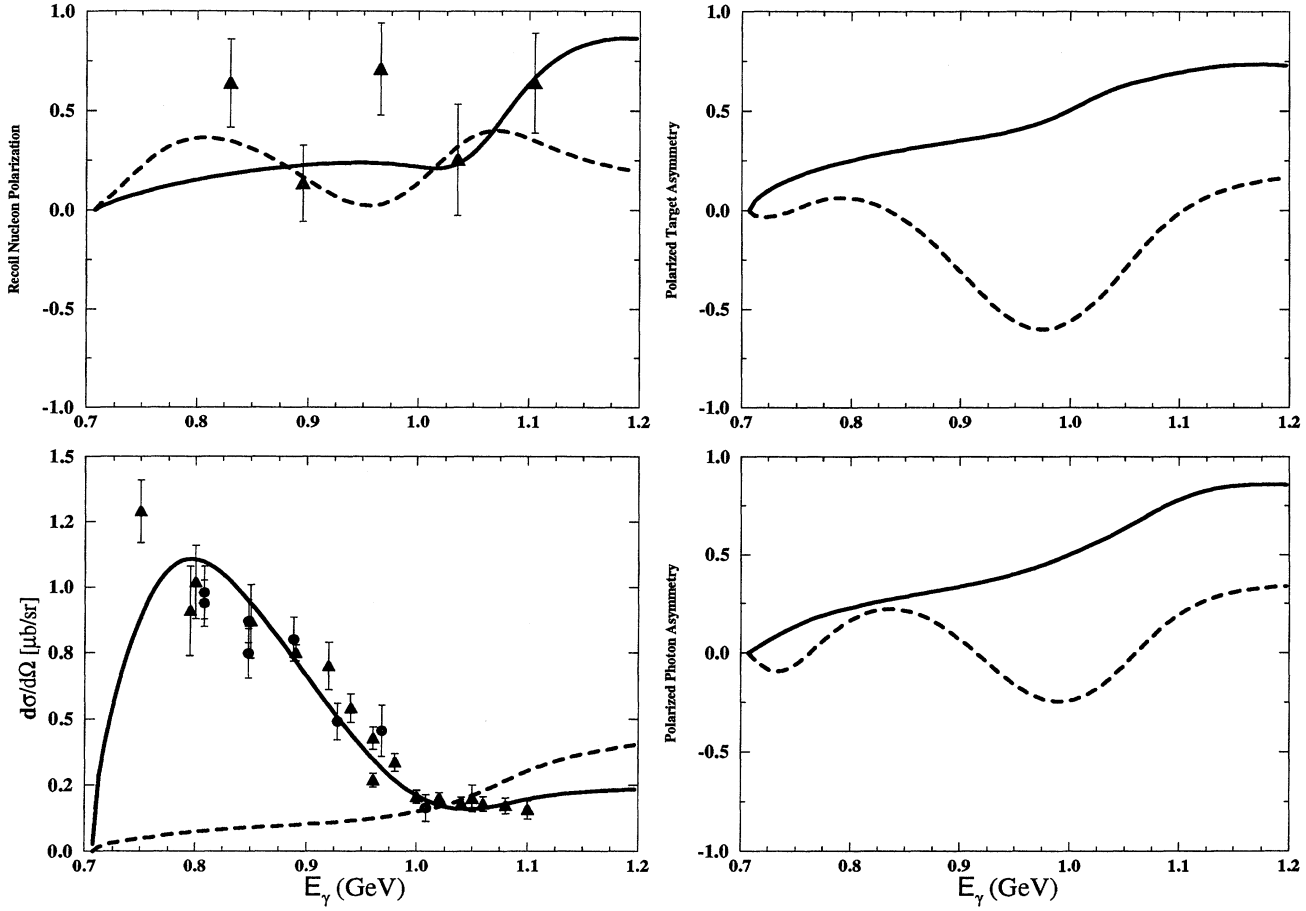

FIG. 2. Differential cross section and recoil nucleon polarization at c.m. angle of $90° \pm 9°$ for the reaction $\gamma p \to \eta p$ as a function of the photon lab energy, a typical example from the "old" data set. The data sets of Homma *et al.* [26] are marked with circles. The dots correspond to the older data [23]. Fit A, shown by the solid lines, uses the PDG92 resonance parameters. The dashed curve excludes the $N^*(1535)$ contribution. Predicted polarized target and photon asymmetries, for which there are no data, are also shown.

toproduction data have not only suffered from the crudeness of the data, but also from the lack of enough theoretical constraints in restricting the number of parameters fitted, *24 or more.* The effective Lagrangian provides us with a *tremendous reduction* in the number of free parameters, *eight in the present work.* The data base is immensely improved with the addition of the Bates and Mainz data sets, the latter still in their preliminary form.

(4) The E_{0+} amplitude at the η photoproduction threshold, inferred from the new Bates data, does not agree with those extracted from the older data set and the new Mainz data. However, the conclusions on the $N^*(1535)$ excitation amplitude are similar in analyses of all of these data sets.

(5) Our analysis yields a *precise estimate* of the product $\Gamma_\eta^{1/2} A_{1/2}$ for the $N^*(1535)$, which is quite insensitive to the uncertainties in the other resonance properties known thus far. For a given set of these resonance parameters, it is *not sensitive* to the detail of the background, such as the off-shell parameters of $N^*(1520)$, the form factor in the vector meson amplitude, and the type of the meson-nucleon coupling.

(6) The present experimental situation on photoproduction at higher energies ($W \geq 1400$ MeV) is not precise enough to extract any meaningful information about the contributions from resonances other than the $N^*(1535)$.

We should stress that precise data on the polarization observables are missing and are badly needed. These would be valuable to test the models for the background contributions.

As to the future extension of this work, we must mention the prospect for a rigorous investigation of the unitarity effects. The application of unitarity to the η photoproduction process is a very complicated task, because there are a fair number of channels coupled to the process and many of them contain more than two particles in the final state, as in the case of multipion production channels. Therefore, even a modest unitarization of the amplitude should include at least five channels. There is no consistent partial wave analysis of the chan-

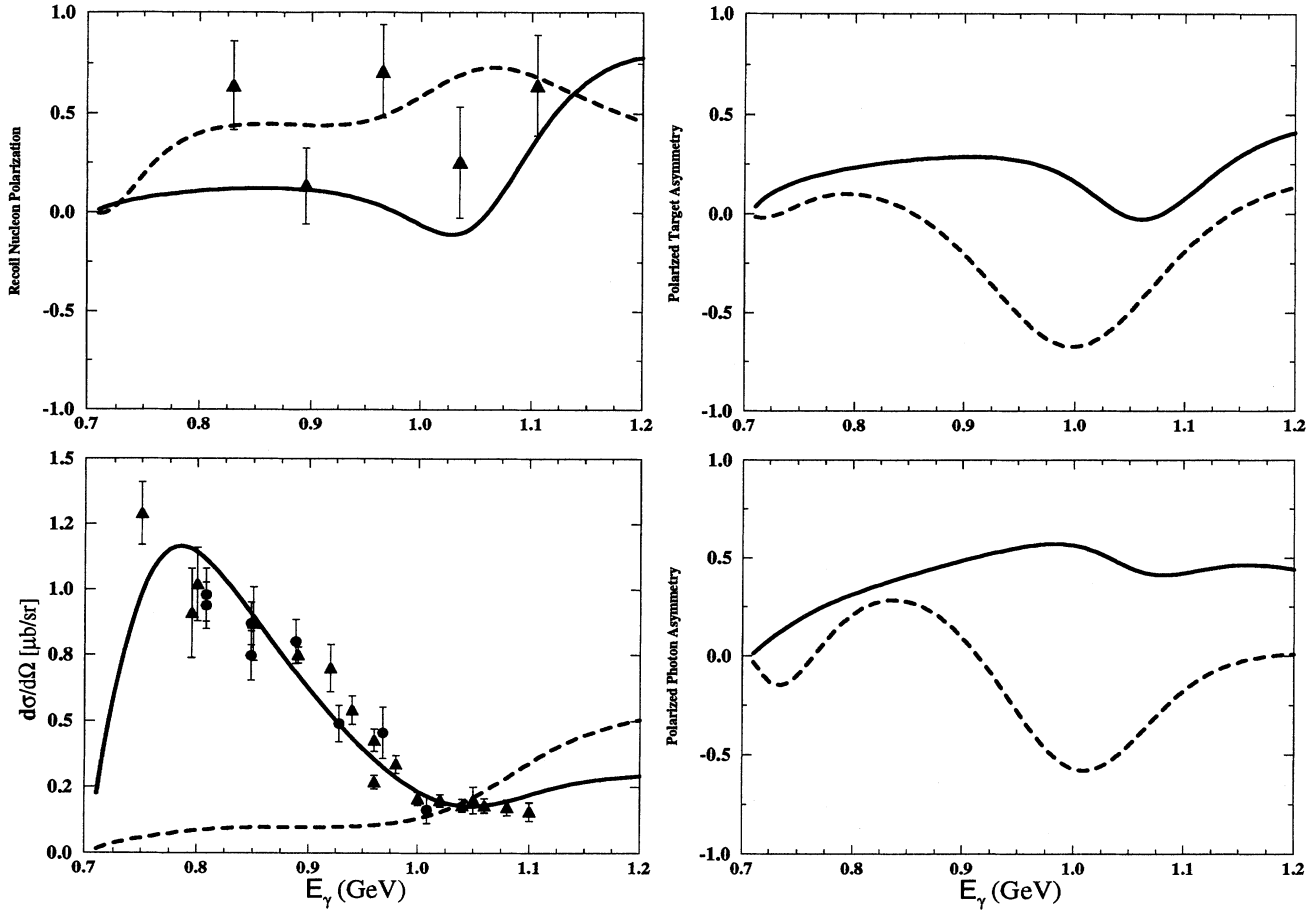

FIG. 3. Calculated observables using the Koch [89] resonance parameters. See Fig. 2 for explanations.

nel, $\pi N \to \eta N$, one of the most important; also, no experimental information on the $\eta N \to \eta N$ process is available. A successful understanding of strong interaction processes will help implement unitarity to electromagnetic processes. Therefore, the pion-induced η production, to be studied at facilities such as COSY in Jülich, Germany, could help a great deal. These could be investigated using the Lagrangians for the strong vertices considered here. Valuable information on the strong decays of the type $N^* \to N\eta$ could be extracted. Existing treatments of these processes give acceptable representation of the data, but do not make any precise connection with hadron models.

An obvious extension of the present analysis is the photoproduction of η' meson on the nucleon, which is underway [98]. A comparative study of η and η' may lead to valuable information on how η and η' interact with nucleons and their excited states.

It is also interesting to use the η photoproduction amplitude as an effective impulse operator to study photoproduction of η mesons off nuclei. Such a theoretical study has been initiated by Doyle [11], and followed by others [33]. One would like to learn more about the properties of the $N^*(1535)$ in the nuclear medium [99]. One important task is to use the effective Lagrangian, developed here, to investigate the photoproduction of the η meson on the deuteron, where there seems to remain a serious discrepancy between the recent theoretical investigation [100] and photoproduction experiments. *This process is very crucial in extracting the electromagnetic transition amplitude of $N^*(1535)$ on the neutron, for which hadron models have clear-cut predictions.*

Hopefully, this paper has provided a good motivation for future work involving physics of η mesons and excited baryons. Careful studies of electromagnetic as well as hadronic η production processes are needed to obtain a more complete picture of the ηN and η-nucleus interactions. New facilities, such as CEBAF and COSY, would be good places to explore this subject further. Particular mention should be made of the superior design capabilities of a device called the CEBAF Large Acceptance Spectrometer (CLAS): its almost 4π solid angle coverage and the possible use of polarized targets and beams in conjunction with it. Our work lays the basic foundation for theoretical analysis which would be indispensable for the studies for photo- and electroproduction of η mesons [101,102] with such spectrometers.

Note added in proof. Since the submission of our paper, the η photoproduction data from Mainz and Bonn [J. W. Price (private communication)] have been presented in various conferences in extensive form. Our preliminary examination of these data bases in newer versions does not alter our conclusions reported here. These two data sets appear mutually compatible, but differ significantly

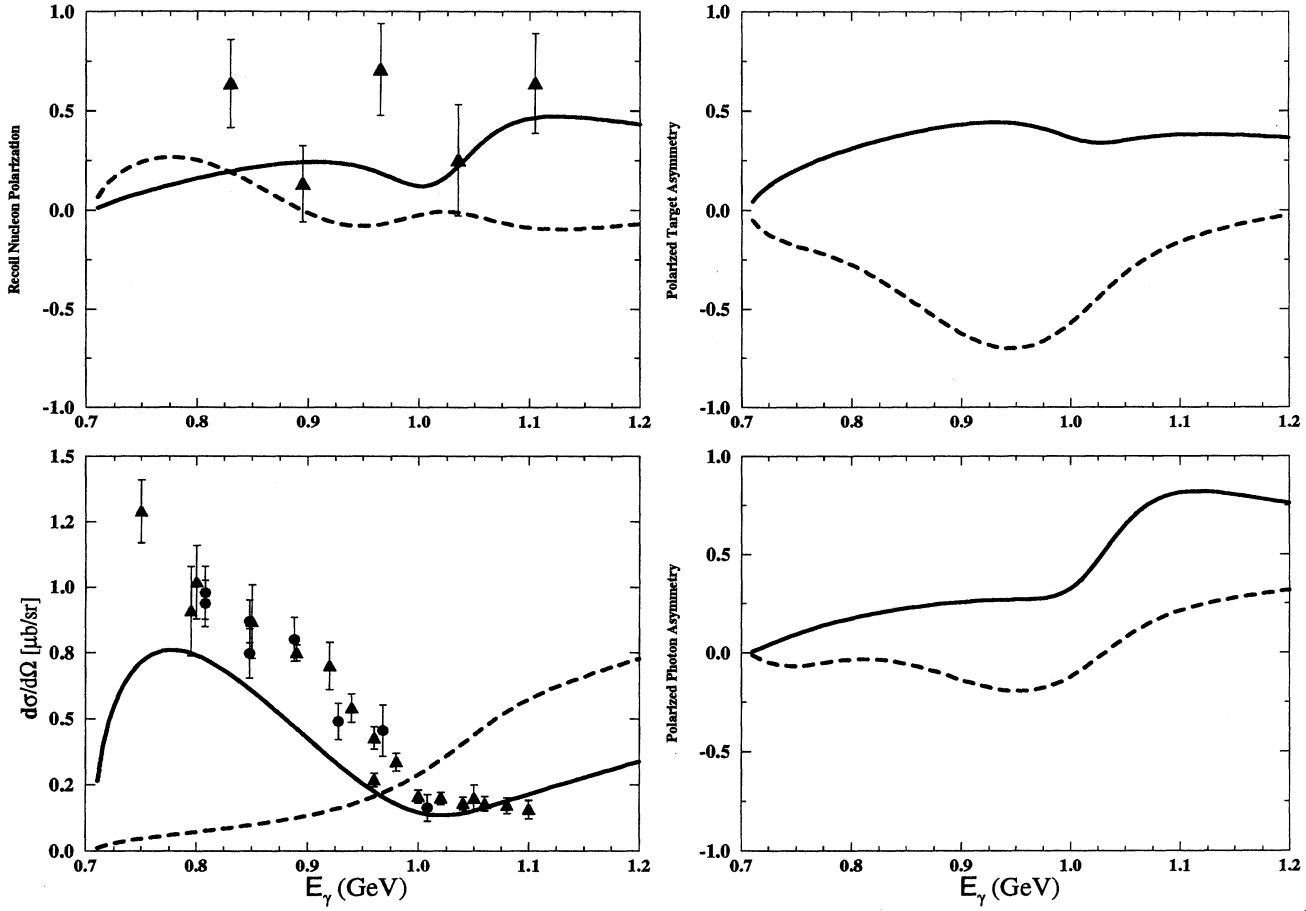

FIG. 4. Calculated observables using the Bakr [78] resonance parameters. See Fig. 2 for explanation.

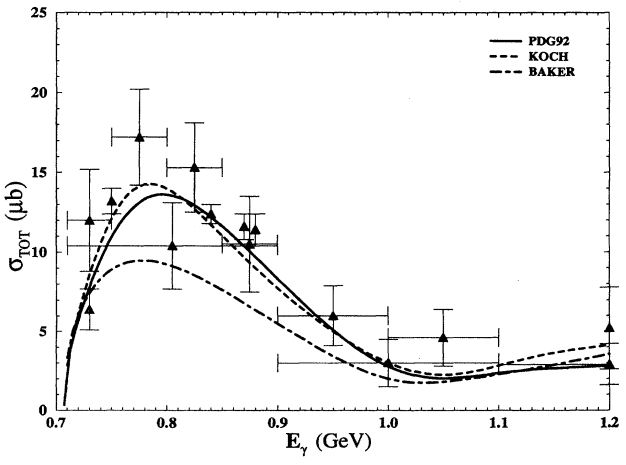

FIG. 5. Predicted total cross section from the Fit A as a function of incident photon lab energy, for the process $\gamma p \to \eta p$. The curves correspond to the different resonance parameters: solid: PDG92, dash: Koch, dotted: Bakr, and data are from Ref. [78].

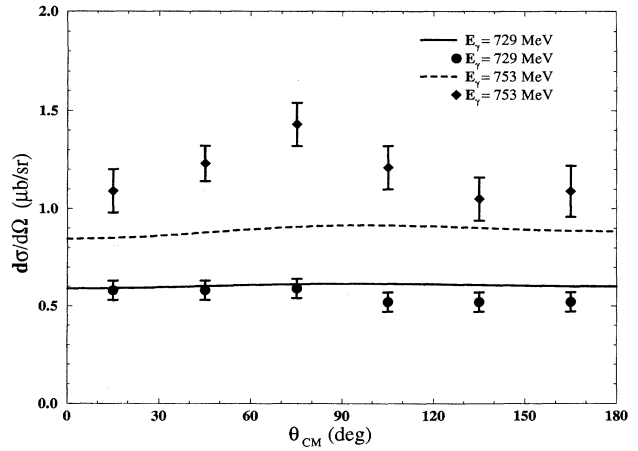

FIG. 6. Predicted angular distributions for the photon lab energy $E_\gamma = 729$ MeV and 753 MeV. The curves correspond to the prediction of the Fit A. The circles and diamonds are the new Bates 1993 data [28].

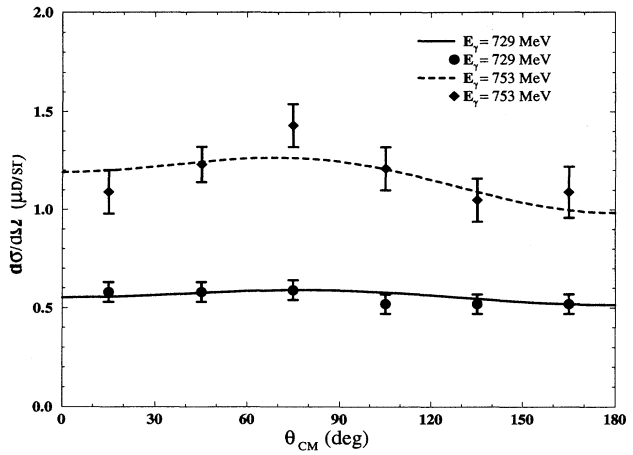

FIG. 7. Predicted angular distributions from our Fit C for $E_\gamma = 729$ MeV and 753 MeV, compared with the Bates data [28].

from the old data base used in our fit A. The latest Mainz data set of 90 data points gives in our approach $\xi = 2.1 \pm 0.1$, instead of Eq. (106), using the same values for α and Λ as in Eq. (106).

ACKNOWLEDGMENTS

We are particularly grateful to R. M. Davidson and L. Zhang for many helpful discussions. We thank many experimental colleagues around the world for their strong interest and input, especially S. Dytman, B. Gothe, B. Krusche, B. Ritchie, B. Schoch, P. Stoler, and H. Stroeher. The research at Rensselaer was supported by the U.S. Department of Energy, while the research at SAL has been supported by the Natural Sciences and Engineering Research Council of Canada. One of us (N.C.M.) thanks D. M. Skopik and E. Tomusiak for their warm hospitality at SAL.

APPENDIX A: RELATION BETWEEN THE CGLN AMPLITUDES AND THE HELICITY AMPLITUDES

In this section, for completeness, we discuss both photo- and electroproduction amplitudes.

In the c.m. system, we quantize the initial and final spins along the directions of $\hat{\mathbf{k}}$ and $\hat{\mathbf{q}}$. We choose the z axis along the photon momentum:

$$\hat{\mathbf{k}} = \frac{\mathbf{k}}{|\mathbf{k}|} = (0,0,1)$$

$$\hat{\mathbf{q}} = \frac{\mathbf{q}}{|\mathbf{q}|} = (\cos\phi\sin\theta, \sin\phi\sin\theta, \cos\theta)\ . \tag{A1}$$

The spinors of the initial and final nucleon are

$$\chi_i^{\uparrow} = \begin{pmatrix} 1 \\ 0 \end{pmatrix}, \quad \chi_i^{\downarrow} = \begin{pmatrix} 0 \\ 1 \end{pmatrix}, \tag{A2}$$

$$\chi_f^{\uparrow} = \begin{pmatrix} \cos\frac{\theta}{2} \\ \sin\frac{\theta}{2}e^{i\phi} \end{pmatrix}, \quad \chi_f^{\downarrow} = \begin{pmatrix} -\sin\frac{\theta}{2}e^{-i\phi} \\ \cos\frac{\theta}{2} \end{pmatrix}, \tag{A3}$$

with

$$\boldsymbol{\sigma}\cdot\hat{\mathbf{k}}\chi_i^{\uparrow\ \downarrow} = \pm\chi_i^{\uparrow\ \downarrow}, \tag{A4}$$

$$\boldsymbol{\sigma}\cdot\hat{\mathbf{q}}\chi_f^{\uparrow\ \downarrow} = \pm\chi_f^{\uparrow\ \downarrow}. \tag{A5}$$

Spin up would correspond, in the c.m. frame, to a negative helicity and vice versa. Explicitly, for the initial and final nucleon we have

$$\chi_{i,f}^{\uparrow\ \downarrow} = |\varrho_{i,f} = \mp 1/2\rangle. \tag{A6}$$

In the case of the virtual photon, we have $k\cdot\varepsilon = 0$; the photon polarization has three independent components. To be consistent with the photoproduction process [86], it is convenient to take two of them to be

$$\varepsilon^{\mu}(\lambda_\gamma) = \frac{1}{\sqrt{2}}(0, -\lambda_\gamma, -i, 0) \qquad \lambda_\gamma = \pm 1. \tag{A7}$$

The third vector is chosen, with the normalization $\varepsilon\cdot\varepsilon = 1$, to be

$$\varepsilon^{\mu}(0) = \frac{1}{\sqrt{-k^2}}(|\mathbf{k}|, 0, 0, k_0). \tag{A8}$$

Using the relations above and defining [86] $A = -i\mathcal{F}$, Eq. (26) becomes

$$A_{\varrho\lambda} = -\frac{1}{\sqrt{2}}(\lambda_\gamma + 2\varrho_i)\left[\cos\frac{\theta}{2}\delta_{\varrho_f,-\varrho_i} - 2\varrho_f\sin\frac{\theta}{2}e^{2i\varrho_f\phi}\delta_{-\varrho_f,-\varrho_i}\right](\mathcal{F}_1 + 4\varrho_f\varrho_i\mathcal{F}_2)$$

$$+\frac{1}{\sqrt{2}}\lambda_\gamma e^{i\lambda_\gamma\phi}\sin\theta\left[\cos\frac{\theta}{2}\delta_{\varrho_f,\varrho_i} - 2\varrho_f\sin\frac{\theta}{2}e^{2i\varrho_f\phi}\delta_{-\varrho_f,\varrho_i}\right](2\varrho_i\mathcal{F}_3 + 2\varrho_f\mathcal{F}_4), \tag{A9}$$

for $\lambda_\gamma = \pm 1$, and

$$A_{\varrho\lambda} = \sqrt{\frac{-k^2}{|\mathbf{k}|}}\left[\cos\frac{\theta}{2}\delta_{\varrho_f,\varrho_i} - 2\varrho_f\sin\frac{\theta}{2}e^{2i\varrho_f\phi}\delta_{-\varrho_f,\varrho_i}\right] \times(2\varrho_f\mathcal{F}_5 + 2\varrho_i\mathcal{F}_6), \tag{A10}$$

for $\lambda_\gamma = 0$, where $\lambda = \lambda_\gamma - \varrho_i$ and $\varrho = -\varrho_f$. By separating the ϕ phase factor, the following helicity amplitudes are defined [105] in the usual manner:

$$H_1 = e^{-i\phi}A_{1/2\,3/2} = -\tfrac{1}{\sqrt{2}}\sin\theta\cos\tfrac{\theta}{2}(\mathcal{F}_3 + \mathcal{F}_4),$$

$$H_2 = A_{1/2\,1/2} = \sqrt{2}\cos\tfrac{\theta}{2}\left\{(\mathcal{F}_2 - \mathcal{F}_1) + \sin^2\tfrac{\theta}{2}(\mathcal{F}_3 - \mathcal{F}_4)\right\},$$

$$
\begin{aligned}
H_3 &= e^{-2i\phi}A_{-1/2\,3/2} = \tfrac{1}{\sqrt{2}}\sin\theta\sin\tfrac{\theta}{2}(\mathcal{F}_3-\mathcal{F}_4),\\
H_4 &= e^{-i\phi}A_{-1/2\,1/2}\\
&= \sqrt{2}\sin\tfrac{\theta}{2}\left\{(\mathcal{F}_2+\mathcal{F}_1)+\cos^2\tfrac{\theta}{2}(\mathcal{F}_3+\mathcal{F}_4)\right\},\\
H_5 &= A_{-1/2\,-1/2} = \sqrt{\frac{-k^2}{|\mathbf{k}|}}\cos\tfrac{\theta}{2}(\mathcal{F}_5+\mathcal{F}_6),\\
H_6 &= e^{i\phi}A_{1/2\,-1/2} = \sqrt{\frac{-k^2}{|\mathbf{k}|}}\sin\tfrac{\theta}{2}(\mathcal{F}_6-\mathcal{F}_5).
\end{aligned}
\tag{A11}
$$

For photoproduction, hereafter, we shall take $\lambda_\gamma = \pm 1$, and the amplitudes H_5 and H_6 to be zero.

APPENDIX B: MULTIPOLES AND HELICITY ELEMENTS

1. Helicity elements

The angular dependence of the $\mathcal{F}_i$ amplitudes, defined in Eq. (25), can be now made explicit through their expansion, in terms of the multipoles and the derivatives of the Legendre polynomials $P_\ell(x)$ of the first kind [51,104,105]:

$$
\begin{aligned}
\mathcal{F}_1 &= \sum_{\ell=0}^{\infty}[\ell M_{\ell+}+E_{\ell+}]P'_{\ell+1}\\
&\quad +[(\ell+1)M_{\ell-}+E_{\ell-}]P'_{\ell-1},\\
\mathcal{F}_2 &= \sum_{\ell=1}^{\infty}[(\ell+1)M_{\ell+}+\ell M_{\ell-}]P'_{\ell},\\
\mathcal{F}_3 &= \sum_{\ell=1}^{\infty}[E_{\ell+}-M_{\ell+}]P''_{\ell+1}+[E_{\ell-}+M_{\ell-}]P''_{\ell-1},\\
\mathcal{F}_4 &= \sum_{\ell=2}^{\infty}[M_{\ell+}-E_{\ell+}-M_{\ell-}-E_{\ell-}]P''_{\ell}.
\end{aligned}
\tag{B1}
$$

We note here the extra amplitudes for electroproduction, $\mathcal{F}_5$ and $\mathcal{F}_6$, given by

$$
\begin{aligned}
\mathcal{F}_5 &= \sum_{\ell=1}^{\infty}[\ell S_{\ell-}-(\ell+1)S_{\ell+}]P'_{\ell},\\
\mathcal{F}_6 &= \sum_{\ell=0}^{\infty}[(\ell+1)S_{\ell+}P'_{\ell+1}-\ell S_{\ell-}P'_{\ell-1}]\ .
\end{aligned}
\tag{B2}
$$

The inverse relations between the multipoles and the c.m. amplitudes $\mathcal{F}_i$ involve projections by angular integration are given by Eq. (B10).

Following Jacob and Wick [106], the angular momentum decomposition of the helicity amplitudes $A_{\mu\lambda}(\theta,\phi)$ is written as [107]

$$
A_{\varrho\lambda}(\theta,\phi) = \sum_J A^J_{\varrho\lambda}(2J+1)d^J_{\lambda\varrho}(\theta)e^{i(\lambda-\varrho)\phi},
\tag{B3}
$$

where θ,ϕ represent the angular direction of the outgoing meson, $\varrho = -\varrho_f$ and $\lambda = \lambda_\gamma - \varrho_i$, with ϱ_f, ϱ_i being the final and initial nucleon helicities and λ_γ the photon helicity. For transverse photons, $\lambda_\gamma = \pm 1$ leads to four possibilities for the initial γN state helicity $\lambda = \pm\frac{1}{2}, \pm\frac{3}{2}$. For scalar photons, $\lambda_\gamma = 0$ and $\lambda = \pm\frac{1}{2}$. In total, there are eight helicity amplitudes $A_{\varrho\lambda}$, but the parity symmetry [106]

$$
A_{-\varrho,-\lambda}(\theta,\phi) = -e^{i(\lambda-\varrho)(\pi-2\phi)}A_{\varrho,\lambda}(\theta,\phi),
\tag{B4}
$$

reduces this number to four. Since the functions $\sqrt{(2J+1)}d^J_{\lambda\varrho}(\theta)e^{i(\lambda-\varrho)\phi}$, for different values of J, are mutually orthogonal and normalized to 4π, when integrated over $d\Omega$, the partial wave helicity amplitudes $A^J_{\varrho,\lambda}$ can be readily deduced from Eq. (B3):

$$
A^J_{\varrho\lambda} = \frac{1}{4\pi}\int d\Omega A_{\varrho\lambda}(\theta,\phi)d^J_{\lambda\varrho}e^{-i(\lambda-\varrho)\phi}.
\tag{B5}
$$

Here $A^J_{\varrho\lambda}$ depends only on the energy and can be combined into four independent partial wave amplitudes, often called helicity elements (proportional to $A^J_{\varrho,\lambda} \pm A^J_{-\varrho,\lambda}$), of good parity and total angular momentum J. These can be defined as

$$
\begin{aligned}
A_{\ell+} &= -\tfrac{1}{\sqrt{2}}(A^J_{1/2,1/2}+A^J_{-1/2,1/2}),\\
A_{(\ell+1)-} &= \tfrac{1}{\sqrt{2}}(A^J_{1/2,1/2}-A^J_{-1/2,1/2}),\\
B_{\ell+} &= \sqrt{\tfrac{2}{\ell(\ell+2)}}(A^J_{1/2,3/2}+A^J_{-1/2,3/2}),\\
B_{(\ell+1)-} &= -\sqrt{\tfrac{2}{\ell(\ell+2)}}(A^J_{1/2,3/2}-A^J_{-1/2,3/2}),\\
C_{\ell+} &= -\tfrac{1}{\sqrt{2}}(A^J_{-1/2,-1/2}+A^J_{1/2,-1/2}),\\
C_{(\ell+1)-} &= \tfrac{1}{\sqrt{2}}(A^J_{-1/2,-1/2}-A^J_{1/2,-1/2})\ ,
\end{aligned}
\tag{B6}
$$

where $\ell\pm$ refer to the two states with η orbital angular momentum ℓ and total angular momentum $J = \ell \pm \frac{1}{2}$. The four helicity elements correspond to transverse photons with helicity $\lambda_\gamma = +1$. The $\lambda_\gamma = -1$ helicity elements are simply related to the $\lambda_\gamma = +1$ via Eq. (B4). The last two helicity elements refer to scalar photons with helicity $\lambda_\gamma = 0$. Equation (B3) can be rewritten in terms of the A's, B's and the derivatives of the Legendre polynomials of the first kind

$$
A_{1/2,1/2}(\theta,\phi) = \sqrt{2}\cos\frac{\theta}{2}\sum_{\ell=0}^{\infty}(A_{(\ell+1)-}-A_{\ell+})(P'_{(\ell+1)}-P'_{\ell}),
$$

$$
A_{-1/2,1/2}(\theta,\phi) = \sqrt{2}e^{i\phi}\sin\frac{\theta}{2}\sum_{\ell=0}^{\infty}(A_{(\ell+1)-}+A_{\ell+})(P'_{(\ell+1)}+P'_{\ell}),
$$

$$A_{1/2,3/2}(\theta,\phi) = \frac{1}{\sqrt{2}}e^{i\phi}\sin\theta\cos\frac{\theta}{2}\sum_{\ell=1}^{\infty}(B_{(\ell+1)-}-B_{\ell+})(P''_{(\ell+1)}-P''_{\ell}),$$

$$A_{-1/2,3/2}(\theta,\phi) = \frac{1}{\sqrt{2}}e^{2i\phi}\sin\theta\sin\frac{\theta}{2}\sum_{\ell=1}^{\infty}(B_{(\ell+1)-}+B_{\ell+})(P''_{(\ell+1)}+P''_{\ell}), \tag{B7}$$

$$A_{-1/2,-1/2}(\theta,\phi) = \sqrt{2}\cos\frac{\theta}{2}\sum_{\ell=0}^{\infty}(C_{(\ell+1)-}-C_{\ell+})(P'_{(\ell+1)}-P'_{\ell}),$$

$$A_{-1/2,+1/2}(\theta,\phi) = -\sqrt{2}e^{-i\phi}\sin\frac{\theta}{2}\sum_{\ell=0}^{\infty}(C_{(\ell+1)-}+C_{\ell+})(P'_{(\ell+1)}+P'_{\ell}). \tag{B8}$$

2. Relations between the multipoles and the helicity elements

The relations between the multipoles and the helicity elements can now be established by substituting Eqs. (B1) and (B2) into Eq. (A11) and comparing the result with relations given by Eq. (B7). Explicitly they are given by

$$\begin{aligned}
A_{\ell+} &= \tfrac{1}{2}[\ell M_{\ell+}+(\ell+2)E_{\ell+}],\\
B_{\ell+} &= E_{\ell+}-M_{\ell+},\\
A_{(\ell+1)-} &= \tfrac{1}{2}[(\ell+2)M_{(\ell+1)-}-\ell E_{(\ell+1)-}],\\
B_{(\ell+1)-} &= E_{(\ell+1)-}+M_{(\ell+1)-},\\
C_{\ell+} &= -\sqrt{\tfrac{-k^2}{2|\mathbf{k}|}}(\ell+1)S_{\ell+}\ ,\\
C_{(\ell+1)-} &= \sqrt{\tfrac{-k^2}{2|\mathbf{k}|}}(\ell+1)S_{(\ell+1)-}.
\end{aligned} \tag{B9}$$

Equations (B1) and (B2) can be inverted to give the multipoles [51]

$$\begin{aligned}
E_{\ell+} &= \tfrac{1}{2(\ell+1)}\int_{-1}^{+1}dx\left[P_\ell\mathcal{F}_1-P_{\ell+1}\mathcal{F}_2+\tfrac{\ell}{2\ell+1}(P_{\ell-1}-P_{\ell+1})\mathcal{F}_3+\tfrac{\ell+1}{2\ell+3}(P_\ell-P_{\ell+2})\mathcal{F}_4\right],\\
E_{\ell-} &= \tfrac{1}{2\ell}\int_{-1}^{+1}dx\left[P_\ell\mathcal{F}_1-P_{\ell-1}\mathcal{F}_2+\tfrac{\ell+1}{2\ell+1}(P_{\ell+1}-P_{\ell-1})\mathcal{F}_3+\tfrac{\ell}{2\ell-1}(P_\ell-P_{\ell-2})\mathcal{F}_4\right],\\
M_{\ell+} &= \tfrac{1}{2(\ell+1)}\int_{-1}^{+1}dx\left[P_\ell\mathcal{F}_1-P_{\ell+1}\mathcal{F}_2-\tfrac{1}{2\ell+1}(P_{\ell-1}-P_{\ell+1})\mathcal{F}_3\right],\\
M_{\ell-} &= \tfrac{1}{2\ell}\int_{-1}^{+1}dx\left[-P_\ell\mathcal{F}_1+P_{\ell-1}\mathcal{F}_2+\tfrac{1}{2\ell+1}(P_{\ell-1}-P_{\ell+1})\mathcal{F}_3\right],\\
S_{\ell+} &= \tfrac{1}{2(\ell+1)}\int_{-1}^{+1}dx\left[P_\ell\mathcal{F}_6+P_{\ell+1}\mathcal{F}_5\right],\\
S_{\ell-} &= \tfrac{1}{2\ell}\int_{-1}^{+1}dx\left[P_\ell\mathcal{F}_6+P_{\ell-1}\mathcal{F}_5\right].
\end{aligned} \tag{B10}$$

APPENDIX C: OBSERVABLES FOR THE η PHOTOPRODUCTION

The η photoproduction observables can be easily obtained in terms of the helicity amplitudes defined in Eq. (A11). They are given by the following standard expressions [86].

(i) Differential cross section:

$$\frac{d\sigma}{d\Omega} = \frac{|\mathbf{q}|}{2|\mathbf{k}|}\sum_{i=1}^{i=4}|H_i|^2. \tag{C1}$$

(ii) Polarized photon asymmetry:

$$\frac{d\sigma}{d\Omega}\Sigma = \frac{|\mathbf{q}|}{|\mathbf{k}|}\mathrm{Re}\{H_1H_4^*-H_2H_3^*\}. \tag{C2}$$

(iii) Recoil nucleon polarization in the direction $\mathbf{k}\times\mathbf{q}$:

$$\frac{d\sigma}{d\Omega}\mathcal{P} = -\frac{|\mathbf{q}|}{|\mathbf{k}|}\mathrm{Im}\{H_1 H_3^* + H_2 H_4^*\}. \tag{C3}$$

(iv) Polarized target asymmetry:

$$\frac{d\sigma}{d\Omega}\mathcal{T} = \frac{|\mathbf{q}|}{|\mathbf{k}|}\mathrm{Im}\{H_1 H_2^* + H_3 H_4^*\}. \tag{C4}$$

APPENDIX D: SPIN-3/2 FIELDS

1. Spin-3/2 propagators

It is useful to discuss some of the important theoretical issues [108,109,110] associated with the treatment of the spin-3/2 baryons. First, the free massive spin-3/2 field is well known to be consistently described by the Lagrangian [111,112]

$$\mathcal{L}_{\text{free}} = \bar{\Psi}^\mu \Lambda_{\mu\nu} \Psi^\nu, \tag{D1}$$

with

$$\Lambda_{\mu\nu} = \Big[(-i\partial_\lambda \gamma^\lambda + M_R) g_{\mu\nu} - iA(\gamma_\mu \partial_\nu + \gamma_\nu \partial_\mu) - \frac{i}{2}(3A^2 + 2A + 1)\gamma_\mu \partial^\lambda \gamma_\lambda \gamma_\nu - M_R(3A^2 + 3A + 1)\Big], \tag{D2}$$

where M_R is the mass of the spin-3/2 baryon and A is an arbitrary parameter subject to the restriction $A \neq -1/2$. Physical properties, such as energy-momentum tensor [113] are independent of the parameter A, chosen to be real here. This is because of the fact that the free Lagrangian Eq. (D1) is invariant under the "point" transformation [114]

$$\Psi^\mu \to \Psi^\mu + a\gamma^\mu \gamma^\nu \Psi_\nu, \tag{D3}$$

$$A \to \frac{A - 2a}{1 + 4a}, \tag{D4}$$

where $a \neq -1/4$, but otherwise arbitrary. Using the Euler-Lagrange equations, the local wave equation for the spin-3/2 field [115] (see also [116,80]) can be derived [117,118]:

$$(i\partial_\mu \gamma^\mu - M_R)\Psi^\nu = 0, \tag{D5}$$

with the subsidiary conditions

$$\gamma_\mu \Psi^\mu = 0, \tag{D6}$$

$$\partial_\mu \Psi^\mu = 0. \tag{D7}$$

Ψ^μ is a sixteen-component Rarita-Schwinger vector spinor. It has a Lorentz vector index μ with a suppressed spinor index which runs from one to four; thus Eqs. (D6) and (D7) imply a sum over the spinor index β:

$$(\gamma_\mu)_{\alpha\beta} \Psi^\mu_\beta = 0. \tag{D8}$$

There are eight constraints coming from Eqs. (D6) and (D7), reducing the number of independent components of Ψ^μ_β to eight (four spin projections for the particle and the other four for the anti-particle).

The propagator for the massive spin-3/2 baryon can be deduced from the equation of motion (see also [119])

$$\Lambda_{\mu\nu} \Psi^\nu = 0. \tag{D9}$$

It satisfies the equation

$$\Lambda_{\mu\lambda} G^\lambda_\nu(x, y) = \delta^4(x - y) g_{\mu\nu}, \tag{D10}$$

where $g_{\mu\nu}$ is the metric tensor. In momentum space,

$$G^\lambda_\nu(x, y) = \int \frac{d^4p}{(2\pi)^4} G^\lambda_\nu(p) e^{-i(x-y)\cdot p}, \qquad \Lambda_{\mu\lambda}(p) G^\lambda_\nu(p) = g_{\mu\nu}. \tag{D11}$$

Solving for G,

$$G_{\mu\nu}(p) = \frac{\gamma \cdot p + M_R}{p^2 - M_R^2}\left[g_{\mu\nu} - \frac{1}{3}\gamma_\mu \gamma_\nu - \frac{1}{3M_R}(\gamma_\mu p_\nu - \gamma_\nu p_\mu) - \frac{2}{3M_R^2} p_\mu p_\nu\right] + \frac{1}{3M_R^2}\frac{A+1}{2A+1}\left[\gamma_\mu p_\nu + \frac{A}{2A+1}\gamma_\nu p_\mu + \left\{\frac{1}{2}\frac{A+1}{2A+1}\gamma \cdot p - \frac{AM_R}{2A+1}\right\}\gamma_\mu \gamma_\nu\right]. \tag{D12}$$

The physical properties of the free field are independent of the parameter A, and we take $A = -1$. This yields the expression for the spin-3/2 propagator:

$$P_{\mu\nu} = \frac{\gamma \cdot p + M_R}{p^2 - M_R^2}\left[g_{\mu\nu} - \frac{1}{3}\gamma_\mu \gamma_\nu - \frac{1}{3M_R}(\gamma_\mu p_\nu - \gamma_\nu p_\mu) - \frac{2}{3M_R^2} p_\mu p_\nu\right]. \tag{D13}$$

We refer the reader to a discussion [80] of erroneous choices of the spin-3/2 propagators adopted by some recent works.

2. Spin projection operators for spin-3/2 field

The spin projection operators are given by [116,80]

$$
\begin{aligned}
(P^{3/2})_{\mu\nu} &= g_{\mu\nu} - \frac{1}{3}\gamma_\mu\gamma_\nu - \frac{1}{3p^2}(\gamma\cdot p\gamma_\mu p_\nu + p_\mu\gamma_\nu\gamma\cdot p),\\
(P^{1/2}_{11})_{\mu\nu} &= \frac{1}{3}\gamma_\mu\gamma_\nu - \frac{p_\mu p_\nu}{p^2}\\
&\quad + \frac{1}{3p^2}(\gamma\cdot p\gamma_\mu p_\nu + p_\mu\gamma_\nu\gamma\cdot p),\\
(P^{1/2}_{22})_{\mu\nu} &= \frac{p_\mu p_\nu}{p^2},\\
(P^{1/2}_{12})_{\mu\nu} &= \frac{1}{\sqrt{3}p^2}(p_\mu p_\nu - \gamma\cdot p\gamma_\mu p_\nu),\\
(P^{1/2}_{21})_{\mu\nu} &= \frac{1}{\sqrt{3}p^2}(\gamma\cdot p\gamma_\nu p_\mu - p_\mu p_\nu).
\end{aligned}
\tag{D14}
$$

These satisfy the orthonormality conditions

$$
(P^I_{ij})_{\mu\lambda}(P^J_{kl})^{\lambda\nu} = \delta^{IJ}\delta_{jk}(P^I_{il})^\nu_\mu, \tag{D15}
$$

and the sum rule for the projection operators

$$
(P^{3/2})_{\mu\nu} + (P^{1/2}_{11})\mu\nu + (P^{1/2}_{22})\mu\nu = g_{\mu\nu}. \tag{D16}
$$

The following properties are also useful:

$$
\gamma\cdot pP^{1/2}_{ij} = \pm P^{1/2}_{ij}\gamma\cdot p, \tag{D17}
$$

$$
\gamma\cdot pP^{3/2} = P^{3/2}\gamma\cdot p, \tag{D18}
$$

where $+$ for $i=j$ and $-$ for $i\neq j$.

APPENDIX E: SPIN-3/2 ISOSPIN-1/2 ODD PARITY CONTRIBUTION TO THE INVARIANT AMPLITUDES

The invariant amplitudes for the s-channel C_1 and C_2 couplings can be expressed in the form

$$
A_i = A_{i,P} + A_{i,NP}. \tag{E1}
$$

The pole (P) and the nonpole (NP) terms for C_1 coupling are given by

$$
\begin{aligned}
A_{1,P} &= \frac{C_1}{8(s-M_R^2)}\left[4t + \frac{4M^2}{3M_R^2}(M_R^2 - M^2 + \mu^2) - \frac{4M}{3M_R}(M_R^2 - M^2 + 2\mu^2)\right],\\
A_{2,P} &= \frac{C_1}{8(s-M_R^2)}[-8],\\
A_{3,P} &= \frac{C_1}{8(s-M_R^2)}\left[-2M + 4M_R - \frac{4M^2}{3M_R} + \frac{2M}{3M_R^2}(M_R^2 - 2M^2 + 2\mu^2)\right],\\
A_{4,P} &= \frac{C_1}{8(s-M_R^2)}\left[6M - 4M_R - \frac{4M^2}{3M_R} + \frac{2M}{3M_R^2}(M_R^2 - 2M^2 + 2\mu^2)\right],
\end{aligned}
\tag{E2}
$$

$$
\begin{aligned}
A_{1,NP} &= \frac{C_1}{12M_R^2}[2M(M-M_R) + \beta(\alpha-1)(s-M^2) - 2\mu^2\beta],\\
A_{2,NP} &= 0,\\
A_{3,NP} &= \frac{C_1}{12M_R^2}[2\alpha\beta M_R - M(\alpha+\beta+\alpha\beta-1)],\\
A_{4,NP} &= \frac{C_1}{12M_R^2}[2\alpha\beta M_R - M(\alpha+\beta+\alpha\beta-1)],
\end{aligned}
$$

with

$$
\alpha = 1+4Z,\quad \beta = 1+4Y,\quad C_1 = \frac{e(k_R^{s,(1)} \pm k_R^{v,(1)})f_{\eta NR}}{2M\mu}. \tag{E3}
$$

The pole and the nonpole terms due to C_2 coupling are

$$
\begin{aligned}
A_{1,P} &= \frac{C_2}{12(s-M_R^2)}\left[2M(3t-2\mu^2) + \frac{1}{M_R}(s+M^2)(s-M^2+\mu^2) - 2M_R(s-M^2)\right],\\
A_{2,P} &= \frac{C_2}{12(s-M_R^2)}[-6(M_R+M)],\\
A_{3,P} &= \frac{C_2}{12(s-M_R^2)}\left[(3t-2\mu^2) + \frac{M}{M_R}(s-M^2+\mu^2) + 5(s-M^2)\right],\\
A_{4,P} &= \frac{C_2}{12(s-M_R^2)}\left[(3t-2\mu^2) + \frac{M}{M_R}(s-M^2+\mu^2) - (s-M^2)\right],
\end{aligned}
\tag{E4}
$$

$$A_{1,NP} = \frac{C_2}{24M_R^2}[(s-M^2)\{M\delta(\alpha-3)+M_R(2\delta\alpha-\alpha-1)\}-4M\mu^2\delta],$$
$$A_{2,NP} = 0,$$
$$A_{3,NP} = \frac{C_2}{24M_R^2}[(s-M^2)(\alpha-1)\delta-2\mu^2\delta],$$
$$A_{4,NP} = \frac{C_2}{24M_R^2}[(s-M^2)(\alpha-1)\delta-2\mu^2\delta],$$

with

$$\alpha = 1+4Z, \quad \delta = 1+2X, \quad C_2 = -\frac{e(k_R^{s,(2)} \pm k_R^{v,(2)})f_{\eta NR}}{4M^2\mu}. \tag{E5}$$

The u-channel invariant amplitudes are obtained from the s-channel ones through crossing relations as given by Eq. (22).

[1] For recent reviews, see N.C. Mukhopadhyay, in *CEBAF Summer 1992 Workshop*, Proceedings, Newport News, Virginia, edited by F. Gross and R. Holt, AIP Conf. Proc. No. 269 (AIP, New York, 1993); N.C. Mukhopadhyay and M. Benmerrouche, in *Future Directions in Particle and Nuclear Physics at Multi-GeV Hadron Beam Facilities*, Proceedings of the Workshop, Upton, New York, 1993, edited by, D.F. Geesaman (BNL Report No. 52389, Upton, 1993).

[2] C. Dover and P. Fishbane, Phys. Rev. Lett. **64**, 3115 (1990).

[3] P. Herczeg, in *Production and Decay of Light Mesons*, Proceedings of the Workshop, Paris, France, 1988, edited by P. Fleury (World Scientific, Singapore, 1988).

[4] O. Dumbrajs *et al.*, Nucl. Phys. **B216**, 277 (1983).

[5] R.S. Bhalerao and L.C. Liu, Phys. Rev. Lett. **54**, 865 (1985).

[6] H.C. Chiang, E. Oset, and L.C. Liu, Phys. Rev. C **44**, 738 (1991), and references therein.

[7] R. Davidson and N.C. Mukhopadhyay, Phys. Rev. Lett. **60**, 748 (1988).

[8] R.M Davidson, N.C. Mukhopadhyay, and R.S. Wittman, Phys. Rev. D **43**, 71 (1991); N.C. Mukhopadhyay and R.M. Davidson, Phys. Rep. (to be published).

[9] R. Wittman and N.C. Mukhopadhyay, Phys. Rev. Lett. **57**, 1113 (1986).

[10] M. Benmerrouche and N.C. Mukhopadhyay, Phys. Rev. D **46**, 101 (1992).

[11] B. Doyle, Ph.D thesis, Rensselaer, 1989.

[12] J. Shaw *et al.*, Phys. Rev. C **43**, 1800 (1991); J.H.J. Distelbrink *et al.*, Phys. Lett. B **271**, 47 (1991); J. Shaw, Ph.D. thesis, Rensselaer, 1994.

[13] M. Benmerrouche and N.C. Mukhopadhyay, Phys. Rev. Lett. **67**, 1070 (1991).

[14] B. Delcourt *et al.*, Phys. Rev. B **29**, 75 (1969).

[15] R. Prepost, D. Lundquist, and D. Quinn, Phys. Rev. Lett. **18**, 82 (1967).

[16] E.D. Bloom *et al.*, Phys. Rev. Lett. **20**, 571 (1968).

[17] C. Bacci *et al.*, Phys. Rev. Lett. **16**, 157 (1966); **16**, 384(E) (1966).

[18] C. Bacci *et al.*, Phys. Rev. Lett. **20**, 571 (1968).

[19] P.S. Booth *et al.*, Lett. Nuovo Cimento **2**, 66 (1969).

[20] C.A. Heusch *et al.*, Phys. Rev. Lett. **17**, 573 (1966).

[21] M. Hongoh *et al.*, Lett. Nuovo Cimento **2**, 66 (1971).

[22] K. Ukai *et al.*, J. Phys. Soc. Jpn. **36**, 18 (1974).

[23] H. Genzel, P. Joos, and W. Pfeil, in *Landolt-Börnstein*, New Series I/8 (Springer, New York, 1973), p. 278.

[24] R. Baldini *et al.*, in *Landolt-Börnstein*, New Series I/12b (Springer, New York, 1988), p. 361.

[25] C.A. Heusch *et al.*, Phys. Rev. Lett. **25**, 1381 (1970).

[26] S. Homma *et al.*, J. Phys. Soc. Jpn. **57**, 828 (1988).

[27] W.W. Daehnick, in *Proceedings of the Conference on Particle Production Near Threshold*, Nashville, Indiana, 1990, edited by Hermann Nann and Edward J. Stephenson, AIP Proc. No. 221 (AIP, New York, 1991), p. 106.

[28] S.A. Dytman *et al.* (private communication).

[29] B. Krusche *et al.* (private communication). [These results have been presented by B. Krusche at many recent international conferences: Trieste, 1993, Perugia, 1993, and Dubna, 1994, and they will appear in the proceedings of these conferences (unpublished).]

[30] H.R. Hicks *et al.*, Phys. Rev. D **7**, 2614 (1973), and references therein.

[31] F. Tabakin, S.A. Dytman, and A.S. Rosenthal, in *Excited Baryons 1988*, Proceedings of the Workshop, Troy, New York, edited by G. Adams, N.C. Mukhopadhyay, and P. Stoler (World Scientific, Teaneck, NJ, 1989).

[32] C. Bennhold and H. Tanabe, Phys. Lett B **243**, 13 (1990).

[33] L. Tiator, C. Bennhold, and S.S. Kamalov, Nucl. Phys. **A580**, 455 (1994).

[34] E. Mazzucato *et al.*, Phys. Rev. Lett. **57**, 3144 (1986).

[35] R. Beck *et al.*, Phys. Rev. Lett. **65**, 1841 (1990).

[36] In this paper, the usual multipole notation [37] has been used.

[37] P. de Baenst, Nucl. Phys. **B24**, 633 (1970), and references therein.

[38] A.N. Kamal, Phys. Rev. Lett. **63**, 2346 (1989).

[39] S. Nozawa, T.S.-H. Lee, and B. Blankleider, Phys. Rev. C **41**, 213 (1990).

[40] L.M. Nath and S.K. Singh, Phys. Rev. C **39**, 1207 (1989).

[41] H.W.L. Naus, Phys. Rev. C **43**, R365 (1991).

[42] V. Bernard, N. Kaiser, and U.-G. Meissner, Phys. Lett. B **282**, 448 (1992).

[43] C.-Y. Ren and M.K. Banerjee, Phys. Rev. C **41**, 2370 (1990).

[44] A.M Bernstein and B.R. Holstein, Comments Nucl. Part. Phys. **20**, 197 (1991).

[45] J. Bergstrom, Phys. Rev. C **44**, 1768 (1991).

[46] Throughout this paper, the Bjorken and Drell conventions [47] on the metric and γ matrices are used. Also,

natural units $\hbar = c = 1$ are used.
[47] J.D. Bjorken and S.D. Drell, *Relativistic Quantum Mechanics* (McGraw-Hill, New York, 1964); *Relativistic Quantum Fields* (McGraw-Hill, New York, 1964).
[48] A. Donnachie, *Photo- and Electroproduction Processes* in *High Energy Physics*, edited by E.H.S. Burhop (Academic, New York, 1972), Vol. V. p. 1.
[49] P. Dennery, Phys. Rev. **124**, 2000 (1961).
[50] G.F. Chew, M.L. Goldberger, F.E. Low, and Y. Nambu, Phys. Rev. **106**, 1345 (1957).
[51] F.A. Berends, A. Donnachie, and D.L. Weaver, Nucl. Phys. **B4**, 103 (1967).
[52] A. Donnachie and G. Shaw, *Electromagnetic Interactions of Hadrons* (Plenum, New York, 1978), Vol. 1, p. 143.
[53] M.L. Goldberger and K.M. Watson, *Collision Theory* (Wiley, New York, 1964); G. v. Gehlen, Nucl. Phys. **B9**, 17 (1969); B.H. Bransden and R.G. Moorhouse, *The Pion-Nucleon System* (Princeton University Press, Princeton, NJ, 1973).
[54] M.G. Olsson and E.T. Osypowski, Nucl. Phys. **B87**, 399 (1975); Phys. Rev. D **17**, 174 (1978); M.G. Olsson, E.T. Osypowski, and E.H. Monsay, *ibid.* **17**, 2938 (1978).
[55] R.D. Peccei, Phys. Rev. **176**, 1812 (1968); **181**, 1902 (1969).
[56] M. Gell-Mann, R.J. Oakes, and B. Renner, Phys. Rev. **175**, 2195 (1968).
[57] A. Manohar and H. Georgi, Nucl. Phys. **B234**, 189 (1984).
[58] U.-G. Meissner, Prog. Theor. Phys. **56**, 903 (1993).
[59] K. Maltman and T. Goldman, Nucl. Phys. **A572**, 682 (1994).
[60] J. Gasser and H. Leutwyler, Ann. Phys. (N.Y.) **158**, 142 (1984).
[61] V. Bernard, N. Kaiser, and U.-G. Meissner, Nucl. Phys. **B383**, 442 (1992).
[62] F. Gross, J.W. Van Orden, and K. Holinde, Phys. Rev. C **41**, R1909 (1990).
[63] H. Genz, M. Nowakowski, and D. Woitschitzky, Phys. Lett. B **250**, 143 (1990); D. Coffman *et al.*, Phys. Rev. D **38**, 2695 (1988).
[64] F. Iachello, N.C. Mukhopadhyay, and L. Zhang, Phys. Rev. D **44**, 898 (1991).
[65] J.C. Peng, *Experiments on η-meson Production*, AIP Conf. Proc. No. 133 (AIP, New York, 1985), p. 255, and references therein.
[66] M.M. Nagels *et al.*, Nucl. Phys. **B147**, 189 (1979).
[67] R. Machleidt, K. Holinde, and Ch. Elster, Phys. Rep. **149**, 1 (1987).
[68] S.N. Gupta, Phys. Rev. **151**, 1235 (1966).
[69] J.L. Friar and B.F. Gibson, Phys. Rev. C **15**, 1779 (1977).
[70] Since the anomalous magnetic moments couple to $F_{\mu\nu}$, gauge invariance is always preserved in the magnetic interaction terms, even with form factors.
[71] D. Schwela and R. Weizel, Z. Phys. **221**, 71 (1969); R. Dolen, D. Horn, and C. Schmid, Phys. Rev. **166**, 1768 (1968).
[72] G. Höhler and E. Pietarinen, Nucl. Phys. **B95**, 210 (1975).
[73] W. Grein and P. Kroll, Nucl. Phys. **A338**, 332 (1980).
[74] S.I. Dolinsky *et al.*, Z. Phys. C **42**, 511 (1989).
[75] S. Godfrey and N. Isgur, Phys. Rev. D **32**, 189 (1985).
[76] G.E. Brown, in *Excited Baryons 1988* [31], p. 17.
[77] J. Feltesse *et al.*, Nucl. Phys. **B93**, 242 (1975).
[78] R.D. Baker *et al.*, Nucl. Phys. **B156**, 93 (1979).
[79] Particle Data Group (PDG), K. Hikasa *et al.*, Phys. Rev. D **45**, S1 (1992), p.I.l; J. J. Hernández *et al.*, Phys. Lett. B **239**, 1 (1990); Rev. Mod. Phys. **48**, S157 (1976).
[80] M. Benmerrouche, R.M. Davidson, and N.C. Mukhopadhyay, Phys. Rev. C **39**, 2339 (1989), and references therein.
[81] M. Gourdin and Ph. Salin, Nuovo Cimento **27**, 193 (1963).
[82] S. Kamefuchi, L. O'Raifeartaigh, and A. Salam, Nucl. Phys. **28**, 529 (1961).
[83] L.M. Nath and B.K. Bhattacharyya, Z. Phys. C **5**, 9 (1980).
[84] M. Fierz and W. Pauli, Proc. R. Soc. London **A173**, 211 (1939).
[85] A.N. Mitra and M. Ross, Phys. Rev. **158**, 1630 (1967); L.A. Copley, G. Karl, and E. Obryk, Nucl. Phys. **B13**, 303 (1969).
[86] R.L. Walker, Phys. Rev. 182, 1729 (1969).
[87] R. Koniuk and N. Isgur, Phys. Rev. D **21**, 1868 (1980).
[88] S. Capstick, Phys. Rev. D **46**, 2864 (1992); S. Capstick and W. Roberts, *ibid.* **49**, 4570 (1994).
[89] R. Koch, in *Baryon 1980*, Proceedings of the IVth International Conference on Baryon Resonances, Toronto, Canada, 1980, edited by N. Isgur (University of Toronto, Toronto, 1980), p. 3.
[90] R.E. Cutkosky, in *Baryon 1980* [89], p. 19.
[91] The quoted error is because of the change of the $\chi^2/N_{\rm DF}$ by 1. If instead the total χ^2 is used, the errors given by MINUIT are much smaller and are not quoted here.
[92] D.M. Manley and E.M. Saleski, Phys. Rev. D **45**, 4002 (1992).
[93] R.P. Feynman, M. Kislinger, and F. Ravndal, Phys. Rev. D **3**, 2706 (1971); F. Ravndal, in *Baryons '92*, Proceedings of the Conference on the Structure of Baryons and Related Mesons, New Haven, Connecticut, edited by M. Gai (World Scientific, Singapore, 1993).
[94] F.E. Close and Z. Li, Phys. Rev. D **42**, 2194, 2207 (1990).
[95] M. Warns, H. Schröder, W. Pfeil, and H. Rollnick, Z. Phys. C **45**, 613, 627 (1990); M. Warns, W. Pfeil, and H. Rollnick, Phys. Rev. D **42**, 2215 (1990).
[96] M. Bourdeau and N.C. Mukhopadhyay, Phys. Rev. Lett. **58**, 976 (1987); **63**, 335 (1989).
[97] C. Carlson and N.C. Mukhopadhyay, Phys. Rev. Lett. **67**, 3745 (1991); Z. Li, V. Burkert, and Z. Li, Phys. Rev. D **46**, 70 (1992).
[98] J.F. Zhang, N.C. Mukhopadhyay, and M. Benmerrouche, Bull. Am. Phys. Soc. **39**, 1092 (1994).
[99] R.C. Carrasco, Phys. Rev. C **48**, 2333 (1993); A. Bianconi, S. Boffi, and D.E. Kharzeev, *ibid.* **49**, R1243 (1994); M.M. Giannini and E. Santopinto, *ibid.* **49**, R1258 (1994); V. A. Tryasuchev, Phys. Atom. Nucl. **57**, 379 (1994).
[100] D. Halderson and A.S. Rosenthal, Nucl. Phys. **A501**, 856 (1989).
[101] S.A. Dytman *et al.*, CEBAF Experiment Proposal No. PR-89-039 (unpublished).
[102] B.G. Ritchie *et al.*, CEBAF Research Proposal, October 1, 1991 (unpublished); and (private communication).
[103] H. Pagels, Phys. Rep. **16**, 219 (1975).
[104] N. Zagury, Phys. Rev. **145**, 1112 (1966); **150**, 1406 (1966); **165**, 1934 (1967); Nuovo Cimento A **52**, 506

(1967).
[105] D.H. Lyth, in *Electromagnetic Interactions of Hadrons*, edited by A. Donnachie and B. Shaw (Plenum, New York, 1978), p. 159.
[106] M. Jacob and G.C. Wick, Ann. Phys. (N.Y.) **7**, 404 (1959).
[107] E. Amaldi, S. Fubini, and G. Furlan, *Pion Electroproduction*, Springer Tracts in Modern Physics 83, edited by G. Hohler (Springer-Verlag, Berlin, 1979).
[108] H. Umezawa, *Quantum Field Theory* (North-Holland, Amsterdam, 1956).
[109] D. Lurie, *Particle and Fields* (Interscience, New York, 1968).
[110] H. Pilkuhn, *The Interactions of Hadrons* (North-Holland, Amsterdam, 1967).
[111] P.A. Moldauer and K.M. Case, Phys. Rev. **102**, 279 (1956).
[112] C. Fronsdal, Suppl. Nuovo Cimento **9**, 416 (1958).
[113] L.M. Nath, B. Etemadi, and J.D. Kimel, Phys. Rev. D **3**, 2153 (1971).
[114] K. Johnson and E.C.G. Sudarshan, Ann. Phys. (N.Y.) **13**, 126 (1961).
[115] In the literature, there is a discussion of a nonlocal wave equation for spin-3/2 field, but such an equation has been rejected because of singularities [116].
[116] P. van Nieuwenhuizen, Phys. Rep. **68**, 189 (1981).
[117] W. Rarita and J. Schwinger, Phys. Rev. **60**, 61 (1941).
[118] A. Aurillia and H. Umezawa, Phys. Rev. **182**, 1682 (1969).
[119] S. Weinberg, Phys. Rev. **133**, B1318 (1964); **134**, B882 (1964).